Fault diagnosis of rolling element bearing based on symmetric cross entropy of neutrosophic sets

Anil Kumar [a,b], C.P. Gandhi [c], Yuqing Zhou [a], Hesheng Tang [a], Jiawei Xiang [a,*]

[a] College of Mechanical and Electrical Engineering, Wenzhou University, Wenzhou 325 035, China
[b] Amity University, Uttar Pradesh 201 313, India
[c] Rayat Bahra University, Mohali 140 104, India

ARTICLE INFO

ABSTRACT

A novel symmetric single-valued neutrosophic cross entropy (SVNCE) measure based upon a newly developed symmetric measure of fuzzy cross entropy is established and then applied it for identifying defects of bearings installed in a test rig and axial piston pump. A 3-level wavelet packet transformation (WPT) is used for extracting and decomposing the fault features associated with the vibrational signals. The new evaluated SVNCE values between knowledge of various faults types and real testing samples provide useful evaluation information of fault types. The concluded results reveal that the proposed SVNCE measure furnishes better fault identification accuracy when compared with the existing model based upon correlation coefficient of simplified neutrosophic sets (SNSs). Furthermore, the proposed SVNCE measure offers consistent and feasible results and is capable for holding the optimal fault type selection under sensitive analysis.

1. Introduction

Over the past few years, various fault diagnosis techniques such as fuzzy approach, neural network, expert system, etc., have been developed and exemplified by eminent researchers [1–12]. Kumar and Kumar [8] developed an adaptive fault diagnosis method for identifying bearing defects. Wang et al. [9] applied empirical wavelet transform for the diagnosis of rolling element defect. Zaire et al. [10] decomposed the vibration signals into intrinsic mode functions (IMFs) and then measured the irregularity and stability of the signals by calculating fuzzy entropy of each IMFs. Fu et al. [11] combined wavelet transform with approximate entropy to detect and diagnose bearing faults during power swings. Based upon wavelet entropy, Yu et al. [12] defined instantaneous entropy and used it to identify various sensor faults on a real micro gas turbine engine. Stief et al. [13] applied principal component analysis and Bayesian sensor fusion for the diagnosis of bearing defect in induction motor. Głowacz and Głowacz [14] explored classification methods such as nearest mean (NM) classifier, Linear discriminant analysis (LDA), and backpropagation neural network (BNN) for the defect diagnosis of commuter motor. Bandit and Pompe [15] used the concept of permutation entropy for analyzing the complexity and irregularity

of vibration signals. Tian et al. [16] proposed an approach based upon permutation entropy for decomposing the non-linear and non-stationary vibration signals in self-adaptive diagnosis of faults in bearings. Zhao et al. [17] proposed multi-scale permutation entropy calculated from signals decomposed by WPT for identifying bearing defects. Cuong [18] introduced and characterized picture fuzzy sets (PFSs) to measure uncertainty in terms of positive, neutral and negative degree membership respectively. Smarandache [19] extended the classical sets theory and introduced a new class of neutrosophic sets (NS) based on true, indeterminacy and falsity membership degree. Weng and Yehang [20] presented a new approach for calculating the similarity between two SVNSs using Dempster-Shafer evidence theory. Recently, Shi [21] introduced a new formula of correlation coefficient based on SNSs and combined it with WPT and then applied it for identifying defects of bearings.

Many times, neural network technique [3,22,23] fails to provide semantic output as it is difficult to understand transferred data stored in its network memory. The expert system technique has some intrinsic shortcomings such as the difficulty of maintaining a database and acquiring knowledge [7]. Fuzzy entropy [10] has been found heavily dependent on its membership function, which is difficult to be accurately determined in real engineering problems. Approximate entropy [11], on another hand, is defective because of its lower estimation value. Permutation entropy [17] is also not a good tool to reveal the real characteristics dealing with

intrinsic time scales of the vibration signals. The approach based on neutrosophic sets (NS) theory is also not suitable for capturing the undetermined, inconsistent and imprecise information for solving real engineering problems. Due to ambiguity and vagueness in the information data, the conventional and existing approaches based upon fuzzy, instantaneous, approximate as well as permutation entropies have been found unsuitable for providing an accurate and quantitative relationship between fault characteristics and fault types.

The fuzzy cross entropy proposed by Bhandari and Pal [24] and Shang and Jiang [25] respectively may not always be suitable for developing further mathematical treatments in certain situations where either their membership functions may produce undefined or meaningless results or indicate an asymmetrical phenomenon. She and Ye [26] concluded that the new cosine similarity measure based on vague sets can reveal more information than the existing cosine similarity measure in dealing with complex and uncertainty problems. To tackle these shortcomings and limitations and to make the applicability of information measures more practical, a novel SVNCE measure based upon a newly established measure of symmetric fuzzy cross entropy is developed and then applied it for diagnosing defects of bearings installed in a test rig and axial piston pump. The advantage of the symmetric nature of the proposed SVNCE measure is that it can be used more suitably for further mathematical treatments in certain situations where membership function of an asymmetrical phenomenon may produce undefined or meaningless results. The rest of this paper is organized as follows.

Section 2 addresses some basic concepts required for the subsequent development of the proposed work. Section 3 provides the data acquisition techniques based on 3-level wavelet packet transformation. Section 4 deals with the development of a novel SVNCE measure between two SVNSs based upon a new symmetric measure of fuzzy cross entropy between two FSs. The next Section 5 validates the feasibility and applicability of the proposed SVNCE measure in details by identifying faults of some rolling bearing elements installed in a test rig and axial piston pump. Furthermore, it compares the fault identification accuracy of the proposed measure with the well-established prediction model based upon SNSs [16]. Finally, Section 6 summarizes the concrete conclusions of the research work done in this paper.

2. Preliminaries

Def. 2.1 A SVNS set. Let $x_1, x_2, ..., x_n$ denotes the generic elements of the universe of discourse X, then, a SVNS $A \subseteq X$ can be defined as $A = \left\{ < x, {}_A\tilde{\mu}(x), {}_A\tilde{i}(x), {}_A\tilde{f}(x) > \forall x \in X \right\}$ where ${}_A\tilde{\mu}(x), {}_A\tilde{i}(x), {}_A\tilde{f}(x)$ represent a truth, an indeterminacy and falsity membership functions respectively and each ${}_A\tilde{\mu}(x), {}_A\tilde{i}(x), {}_A\tilde{f}(x) : X \to [0, 1]$ satisfy $0 \leq {}_A\tilde{\mu}(x) + {}_A\tilde{i}(x) + {}_A\tilde{f}(x) \leq 3$.

Def. 2.2 Algebra of SVNSs: – Any two SVNSs A and B in X satisfy the following laws:

$(i) A \cup B = \left\{ < x, \text{Max.}\left\{ {}_A\tilde{\mu}(x), {}_B\tilde{\mu}(x) \right\}, \text{Max.}\left\{ {}_A\tilde{i}(x), {}_B\tilde{i}(x) \right\}, \text{Max.}\left\{ {}_A\tilde{f}(x), {}_B\tilde{f}(x) \right\} > \right\}$

$(ii) A \cap B = \left\{ < x, \text{Min.}\left\{ {}_A\tilde{\mu}(x), {}_B\tilde{\mu}(x) \right\}, \text{Min.}\left\{ {}_A\tilde{i}(x), {}_B\tilde{i}(x) \right\}, \text{Min.}\left\{ {}_A\tilde{f}(x), {}_B\tilde{f}(x) \right\} > \right\}$

$(iii) A \subseteq B \iff {}_A\tilde{\mu}(x) \leq {}_B\tilde{\mu}(x), {}_A\tilde{i}(x) \geq {}_B\tilde{i}(x) \text{ and } {}_A\tilde{f}(x) \geq {}_B\tilde{f}(x).$

$(iv) A^c = \left\{ < x, {}_A\tilde{f}(x), 1 - {}_A\tilde{i}(x), {}_A\tilde{\mu}(x) > \right\}$

(iv) Two SVNSs are equal, written as $A = B$ iff $A \subseteq B$ and $B \subseteq A$.

Def. 2.3 A measure of neutrosophic entropy. Let $P(X)$ denotes the family of all neutrosophic subsets of the finite universe X, then

a function ${}_NH(A) : P(X) \to R$ is said to be a measure of neutrosophic entropy iff

$(i) {}_NH(A) \geq 0$ $(ii) {}_NH(A) = 0$ iff   either ${}_A\tilde{\mu}(x) = 1, {}_A\tilde{i}(x) = 0, {}_A\tilde{f}(x) = $ 0 or ${}_A\tilde{\mu}(x) = 0, {}_A\tilde{i}(x) = 0, {}_A\tilde{f}(x) = 1$ $(iii) {}_NH(A^c) = {}_NH(A)$

(iv) It should have a maximum value which arises when ${}_A\tilde{\mu}(x) = {}_A\tilde{i}(x) = {}_A\tilde{f}(x) = \frac{1}{2}$ and it should be an increasing function of n

(v) ${}_NH(A)$ must be concave for all ${}_A\tilde{\mu}(x), {}_A\tilde{i}(x), {}_A\tilde{f}(x)$.

Def. 2.4 A fuzzy cross entropy measure. A function $D : P(X) \times P(X) \to R$ is called a measure of fuzzy cross entropy iff

$(i) D(A, B)$ is non-negative for each fuzzy sets $A, B \in X$ with equality iff $A = B$

(ii) $D(A, B)$ should be a convex function of both $A, B \in X$

$(iii) D(A, F) = \text{Max.}\{H(A)\} - H(A)$, where F denotes the fuzziest set and $H(A)$ is the corresponding measure of fuzzy entropy.

Def. 2.5 A symmetric fuzzy cross entropy measure. A function $D : P(X) \times P(X) \to R$ is said to be a symmetric measure of fuzzy cross entropy iff it satisfies (i) and (ii) of def. 2.4 along with (iii) $D(A, B)$ is symmetric in nature, that is $D(A, B) = D(B, A)$ (iv) $D(A^c, B^c) = D(A, B)$. that is $D(A, B)$ should not change whenever the fuzzy sets A and B are replaced by their complements.

Def. 2.6 Minimum and maximum argument principle. Suppose the knowledge of fault types experienced by some rolling bearing can be represented by the set $A = (A_1, A_2, ...A_m), m \in Z^+$. Let the real testing samples to be recognized, can also be represented by the form of a SVNS F_T. Then, the minimum argument principle states that the diagnosing sample A_K should be the nearest one to F_T, that is ${}_{SVNS}K(A_K, F_T) = \text{Min.} {}_{SVNS}K(A_i, F_T)(i = 1, 2, ...m)$, where ${}_{SVNS}K(A_i, F_T)$ represents the discrimination degree of the SVNS A_i from F_T. That is, the real testing sample F_T belongs to the diagnosing sample A_K where $K = \text{Arg.Min.} {}_{SVNS}K(A_i, F_T)$. Furthermore, the maximum argument principle states that the diagnosing sample A_K should be the farthest one to F_T, that is ${}_{SNS}M(A_K, F_T) = \text{Max.} {}_{SNS}M(A_i, F_T)(i = 1, 2, ...m)$ where ${}_{SNS}M(A_i, F_T)$ represents the correlation coefficient of the SNSs A_i and F_T. That is, the real testing sample F_T should belong to the diagnosing sample A_K where $K = \text{Arg.Max.} {}_{SNS}M(A_i, F_T)$.

3. Development of a novel SVNCE measure for identifying bearing defects

In this section, an effort has been made for establishing a new measure of fuzzy entropy, intended to develop a novel measure of symmetric fuzzy cross-entropy as presented in the following two **Theorems 3.1** and **3.2**.

3.1 Theorem. Show that ${}_F\tilde{H}(A) = \sum_{i=1}^{n} \log_{\frac{3}{2}}\left[1 + \frac{1}{4}\sqrt{{}_A\tilde{\mu}(x_i)\left(1 - {}_A\tilde{\mu}(x_i)\right)}\right]$ is a valid measure of fuzzy entropy with minimum value zero and maximum value as $\left(2 - \log_{\frac{3}{2}}2\right)n$.

Proof. (i) Clearly ${}_F\tilde{H}(A) \geq 0$ with equality iff ${}_A\tilde{\mu}(x_i) = 0$ or 1.

(ii) ${}_F\tilde{H}(A)$ remains unchanged whenever ${}_A\tilde{\mu}(x_i)$ and $1 - {}_A\tilde{\mu}(x_i)$ are interchanged.

(iii) Concavity: The series on the right-hand side of ${}_F\tilde{H}(A)$ is a positive term series and hence it is uniformly as well as absolutely convergent, which in turn, possesses continuous first and second order partial derivatives w.r.t. ${}_A\tilde{\mu}(x_i)$. Thus, differentiating ${}_F\tilde{H}(A)$ partially w.r.t. ${}_A\tilde{\mu}(x_i)$ yields:

$$\frac{\partial_F \widetilde{H}(A)}{\partial_A \widetilde{\mu}(x_i)} = \frac{1-2_A\widetilde{\mu}(x_i)}{8\log\frac{3}{2}\sqrt{_A\mu^{\sim}(x_i)(1-_A\mu^{\sim}(x_i))}\left(1+\frac{1}{4}\sqrt{_A\mu^{\sim}(x_i)(1-_A\mu^{\sim}(x_i))}\right)};$$

$$\frac{\partial_F^2 \widetilde{H}(A)}{\partial_A^2 \widetilde{\mu}(x_i)} = -\frac{1}{\log\frac{3}{2}}\left[\begin{array}{c} \frac{\left(1-2_A\widetilde{\mu}(x_i)\right)^2}{64_A\widetilde{\mu}(x_i)\left(1-_A\widetilde{\mu}(x_i)\right)\left(1+\frac{1}{4}\sqrt{_A\widetilde{\mu}(x_i)\left(1-_A\widetilde{\mu}(x_i)\right)}\right)^2} \\ +\frac{\left(1-2_A\widetilde{\mu}(x_i)\right)^2}{16\left[_A\widetilde{\mu}(x_i)\left(1-_A\widetilde{\mu}(x_i)\right)\right]^{\frac{3}{2}}\left(1+\frac{1}{4}\sqrt{_A\widetilde{\mu}(x_i)\left(1-_A\widetilde{\mu}(x_i)\right)}\right)} \\ +\frac{1}{4\left[_A\widetilde{\mu}(x_i)\left(1-_A\widetilde{\mu}(x_i)\right)\right]^{\frac{1}{2}}\left(1+\frac{1}{4}\sqrt{_A\widetilde{\mu}(x_i)\left(1-_A\widetilde{\mu}(x_i)\right)}\right)} \end{array}\right] \leq 0$$

for each $_A\widetilde{\mu}(x_i) \in [0,1]$. This validates the concavity of $_F\widetilde{H}(A)$ w.r.t. $_A\widetilde{\mu}(x_i)$. Also, the three-dimensional rotational plot represented by Fig. 1 (Table 1) establishes the concavity property of the proposed fuzzy entropy $_F\widetilde{H}(A)$.

(iv) Because of the concavity of $_F\widetilde{H}(A)$ with respect to $_A\widetilde{\mu}(x_i)$, we should have its maximum value and it arises when $\frac{\partial_F\widetilde{H}(A)}{\partial_A\widetilde{\mu}(x_i)} = 0$ which gives $_A\widetilde{\mu}(x_i) = \frac{1}{2}$. Also,

$$\text{Max. }_F\widetilde{H}(A) =_F \widetilde{H}(A)|_{_A\mu^{\sim}(x_i)=\frac{1}{2}} = n\log\frac{3}{2}\frac{9}{8} = n\left(2-\log\frac{3}{2}2\right).$$

3.2 Theorem. For any two FSs $A, B \in X$ X, $_{FS}K(A,B)$ is a correct symmetric measure of fuzzy cross entropy where

Table 1
Properties of the proposed fuzzy entropy $_F\widetilde{H}(A)$, symmetric fuzzy cross entropy $_{FS}K(A,B)$ and SVNCE measure.

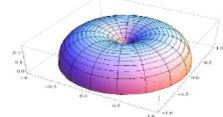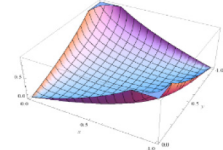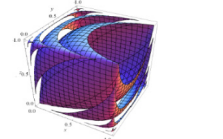| Proposed Measures	Mathematical Formulation	Graphical Representation
Fuzzy Entropy	$_F\widetilde{H}(A)$	Fig. 1. A 3-D rotational plot representing the concavity of $_F\widetilde{H}(A)$
Symmetric Fuzzy Cross Entropy	$_{FS}K(A,B)$	Fig. 2 A 3-D plot representing the max/ min values of $_{FS}K(A,B)$
Single Valued Neutrosophic Entropy	$_N\widetilde{H}(A)$	Fig. 3. A 3-D contour plot representing the min. value of $_N\widetilde{H}(A)$

$$(2+t_1+t_2)\log\frac{3}{2}\left[\frac{2+t_1+t_2}{3+\sqrt{t_1t_2}+t_1+t_2}\right]$$

$$\geq (2+t_1+t_2)\log\frac{3}{2}\left[\frac{2}{3}\right] \text{ for each } t_1,t_2 \in [0,1] \quad (1)$$

$$_{FS}K(A,B) = \sum_{i=1}^{n}\left[\begin{array}{c}\left(2+_A\widetilde{\mu}(x_i)+_B\widetilde{\mu}(x_i)\right)\log\frac{3}{2}\left[\frac{2+_A\widetilde{\mu}(x_i)+_B\widetilde{\mu}(x_i)}{\frac{2}{3}\left[3+_A\widetilde{\mu}(x_i)+_B\widetilde{\mu}(x_i)+\sqrt{_A\widetilde{\mu}(x_i)_B\widetilde{\mu}(x_i)}\right]}\right] \\ +\left(4-_A\widetilde{\mu}(x_i)-_B\widetilde{\mu}(x_i)\right)\log\frac{3}{2}\left[\frac{4-_A\widetilde{\mu}(x_i)-_B\widetilde{\mu}(x_i)}{\frac{2}{3}\left[5-_A\widetilde{\mu}(x_i)-_B\widetilde{\mu}(x_i)+\sqrt{\left(1-_A\widetilde{\mu}(x_i)\right)\left(1-_B\widetilde{\mu}(x_i)\right)}\right]}\right]\end{array}\right]$$

which measures the fuzzy uncertainty between the fuzzy sets A and B.

Proof. It is instructive to note that the conditions (iii) and (iv) of def. 2.5 are straightforward. For the establishment of non-negativity of $_{FS}K(A,B)$, we proceed as follows. For $t_1,t_2 \in [0,1]$, define

$$h(t_1,t_2) = 6 + (2+t_1+t_2)\log\frac{3}{2}\left[\frac{2+t_1+t_2}{3+\sqrt{t_1t_2}+t_1+t_2}\right]$$

$$+ (4-t_1-t_2)\log\frac{3}{2}\left[\frac{4-t_1-t_2}{5-t_1-t_2+\sqrt{(1-t_1)(1-t_2)}}\right]$$

We turn to establish the following lemma, intended to justify the non-negativity condition of the proposed symmetric measure of fuzzy cross entropy.

Lemma 3.1 Let $H_3(t_1,t_2)$ and $A(t_1,t_2)$ denote the Heron's and Arithmetic mean respectively, then there exists the inequality: $H_3(t_1,t_2)$ is less than or equal to $A(t_1,t_2)$ for each $t_1,t_2 \in [0,1]$.

Proof. It is mandatory to subtract the two given expressions of means to yield

$$H_3(t_1,t_2)-A(t_1,t_2) = \frac{t_1+\sqrt{t_1t_2}+t_2}{3}-\frac{t_1+t_2}{2} = -\frac{1}{6}\left(\sqrt{t_1}-\sqrt{t_2}\right)^2 \leq 0$$

The resulting inequality yields

Interchanging t_1,t_2 with their counterparts $(1-t_1),(1-t_2)$ in the foregoing inequality (1) yields

$$(4-t_1-t_2)\log\frac{3}{2}\left[\frac{4-t_1-t_2}{5+\sqrt{(1-t_1)(1-t_2)}-t_1-t_2}\right]$$

$$\geq (4-t_1-t_2)\log\frac{3}{2}\left[\frac{2}{3}\right]\forall t_1,t_2 \in [0,1] \quad (2)$$

With due permission of the foregoing inequalities (1) and (2), we get the following desired result: "For each $t_1,t_2 \in [0,1]$, there exists the inequality $h(t_1,t_2) \geq 0$ with equality iff $h(t_1,t_2) = 0$". Thus, $_{FS}K(A,B) = \sum_{i=1}^{n}h\left(_A\widetilde{\mu}(x_i),_B\widetilde{\mu}(x_i)\right) \geq 0 \forall_A\widetilde{\mu}(x_i),_B\widetilde{\mu}(x_i)$ with equality iff $_A\widetilde{\mu}(x_i) =_B \widetilde{\mu}(x_i)$

The result of following **Theorem 3.3** will put us in a better position to discuss the situation where the newly developed symmetric measure of fuzzy cross entropy $_{FS}K(A,B)$ can assume its maximum and minimum values.

3.3 Theorem. For any two FSs $A,B \in X$, $\exists$ the inequality $0 \leq _{FS}K(A,B) \leq 6\left(2-\log\frac{3}{2}2\right)n$, where n is a fixed integer

Proof. It is informative to note that $_{FS}K(A,B)$ does not change whenever the fuzzy set B is replaced with A^c. Thus,

$$_{FS}K(A, A^c) = \sum_{i=1}^{n} 6\log_{\frac{3}{2}}\left[\frac{3}{\frac{2}{3}\left[4 + \sqrt{_A\mu^{\sim}(x_i)(1 - _A\mu^{\sim}(x_i))}\right]}\right]$$

$$= \sum_{i=1}^{n} 6\log_{\frac{3}{2}}\left[\frac{\frac{9}{8}}{1 + \frac{1}{4}\sqrt{_A\mu^{\sim}(x_i)(1 - _A\mu^{\sim}(x_i))}}\right]$$

$$= \sum_{i=1}^{n}\left[6\log_{\frac{3}{2}}\frac{9}{8} - 6\log_{\frac{3}{2}}\left[1 + \frac{1}{4}\sqrt{_A\widetilde{\mu}(x_i)\left(1 - _A\widetilde{\mu}(x_i)\right)}\right]\right] \tag{3}$$

With the aid of the resulting **Theorem 3.1**, the undergoing equality (3) yields

$$_{FS}K(A, A^c) = 6\left(2 - \log_{\frac{3}{2}}2\right) - _F\widetilde{H}(A) \tag{4}$$

The employment of the non-negative conditions: $_F\widetilde{H}(A) \geq 0$ and $_{FS}K(A,B) \geq 0$ into the undergoing equality (4) yields

$$_F\widetilde{H}(A) = \left(2 - \log_{\frac{3}{2}}2\right)n - \frac{1}{6}{}_{FS}K(A, A^c) \geq 0 \Rightarrow 0 \leq {}_{FS}K\left(A, A^c\right)$$

$$\leq 6\left(2 - \log_{\frac{3}{2}}2\right)n \tag{5}$$

The resulting inequality (5) suggests that $_{FS}K(A, A^c)$ is finite when n is finite. On the same pattern, it can be easily shown that $_{FS}K(A,B)$ satisfies $0 \leq {}_{FS}K(A,B) \leq 6\left(2 - \log_{\frac{3}{2}}2\right)n$. Since the maximum value of $_F\widetilde{H}(A)$ is $\left(2 - \log_{\frac{3}{2}}2\right)n$, (5) suggests that the minimum value of $_{FS}K(A,B)$ is zero. Also, for any crisp set A, i.e., when $_A\widetilde{\mu}(x_i) = 0$ or 1, the minimum value of $_F\widetilde{H}(A)$ is zero and hence the maximum value of $_{FS}K(A,B)$ is $6\left(2 - \log_{\frac{3}{2}}2\right)n$ for a given n and this value is independent on the elements in X and depends only on the cardinality of the universe of discourse X. Also, from three dimensional plot as shown in Fig. 2 (Table 1), it is evident that $_{FS}K(A,B)$ increases as $|A - B|$ increases, attains its maximum value $6\left(2 - \log_{\frac{3}{2}}2\right)n$ at the points (1, 0) and (0, 1) and attains its

minimum value 0 at $A = B$. We now divert our intention to establish one more important theorem, the result of which will play a vital role for developing the desired SVNCE measure.

3.4 Theorem. Show that $_N\widetilde{H}(A)$ is a correct measure of single valued neutrosophic entropy with minimum value zero and maximum value as $3\left(2 - \log_{\frac{3}{2}}2\right)n$ where

$$_N\widetilde{H}(A) = \left(2 - 2\log_{\frac{3}{2}}2\right)n + \sum_{i=1}^{n}\log_{\frac{3}{2}}\left[1 + \frac{1}{4}\sqrt{_A\widetilde{i}(x_i)\left(1 - _A\widetilde{i}(x_i)\right)}\right]$$

$$+ \frac{2 + _A\widetilde{\mu}(x_i) + _A\widetilde{f}(x_i)}{3} \times \log_{\frac{3}{2}}\left[1 + \frac{1 + \sqrt{_A\widetilde{\mu}(x_i)_A\widetilde{f}(x_i)}}{2 + _A\widetilde{\mu}_A(x_i) + _A\widetilde{f}(x_i)}\right] + \sum_{i=1}^{n}$$

$$\times \frac{4 - _A\widetilde{\mu}(x_i) - _A\widetilde{f}(x_i)}{3}\log_{\frac{3}{2}}\left[1 + \frac{1 + \sqrt{\left(1 - _A\widetilde{\mu}(x_i)\right)\left(1 - _A\widetilde{f}(x_i)\right)}}{4 - _A\widetilde{\mu}_A(x_i) - _A\widetilde{f}(x_i)}\right].$$

Proof. The conditions (i), (ii), (iii) and (iv) of **def. 2.3** are obviously true.

Concavity. We can, equally well, repeat the procedure employed in developing the results of **Theorem 3.1** to establish the concavity of $_N\widetilde{H}(A)$ with respect to $_A\widetilde{\mu}(x_i), _A\widetilde{i}(x_i)$ and $_A\widetilde{f}(x_i)$. Thus,

$$\text{Max.}_N\widetilde{H}(A) = \sum_{i=1}^{n}\left(\log_{\frac{3}{2}}\frac{9}{8} + 4\log_{\frac{3}{2}}\frac{3}{2} - 2\log_{\frac{3}{2}}2\right) = 3\left(2 - 2\log_{\frac{3}{2}}2\right)n > 0$$

Also, from the three-dimensional contour plot of the single valued neutrosophic entropy as shown in Fig. 3 (Table 1) it is evident that the minimum value of $_N\widetilde{H}(A)$ is zero.

We now reinterpret the resulting **Theorem 3.4**, intended to develop two more important **Theorems 3.5–3.6**, the results of which will, subsequently, applied for identifying defects of bearings installed in a test rig and axial piston pump.

3.5 Theorem. For any two SVNSs $A, B \in X$, show that $_{SVNS}K(A,B)$ is a correct SVNCE measure represented as

$$_{SVNS}K(A, B) = \sum_{i=1}^{n}\left[\begin{array}{l}\left(2 + _A\widetilde{\mu}(x_i) + _B\widetilde{\mu}(x_i)\right)\log_{\frac{3}{2}}\left[\frac{2 + _A\widetilde{\mu}(x_i) + _B\widetilde{\mu}(x_i)}{\frac{2}{3}\left[3 + _A\widetilde{\mu}(x_i) + _B\widetilde{\mu}(x_i) + \sqrt{_A\widetilde{\mu}(x_i)_B\widetilde{\mu}(x_i)}\right]}\right]\\ + \left(4 - _A\widetilde{\mu}(x_i) - _B\widetilde{\mu}(x_i)\right)\log_{\frac{3}{2}}\left[\frac{4 - _A\widetilde{\mu}(x_i) - _B\widetilde{\mu}(x_i)}{\frac{2}{3}\left[5 - _A\widetilde{\mu}(x_i) - _B\widetilde{\mu}(x_i) + \sqrt{\left(1 - _A\widetilde{\mu}(x_i)\right)\left(1 - _B\widetilde{\mu}(x_i)\right)}\right]}\right]\end{array}\right]$$

$$+ \sum_{i=1}^{n}\left[\begin{array}{l}\left(2 + _A\widetilde{i}(x_i) + _B\widetilde{i}(x_i)\right)\log_{\frac{3}{2}}\left[\frac{2 + _A\widetilde{i}(x_i) + _B\widetilde{i}(x_i)}{\frac{2}{3}\left[3 + _A\widetilde{i}(x_i) + _B\widetilde{i}(x_i) + \sqrt{_A\widetilde{i}(x_i)_B\widetilde{i}(x_i)}\right]}\right]\\ + \left(4 - _A\widetilde{i}(x_i) - _B\widetilde{i}(x_i)\right)\log_{\frac{3}{2}}\left[\frac{4 - _A\widetilde{i}(x_i) - _B\widetilde{i}(x_i)}{\frac{2}{3}\left[5 - _A\widetilde{i}(x_i) - _B\widetilde{i}(x_i) + \sqrt{\left(1 - _A\widetilde{i}(x_i)\right)\left(1 - _B\widetilde{i}(x_i)\right)}\right]}\right]\end{array}\right]$$

$$+ \sum_{i=1}^{n}\left[\begin{array}{l}\left(2 + _A\widetilde{f}(x_i) + _B\widetilde{f}(x_i)\right)\log_{\frac{3}{2}}\left[\frac{2 + _A\widetilde{f}(x_i) + _B\widetilde{f}(x_i)}{\frac{2}{3}\left[3 + _A\widetilde{f}(x_i) + _B\widetilde{f}(x_i) + \sqrt{_A\widetilde{f}(x_i)_B\widetilde{f}(x_i)}\right]}\right]\\ + \left(4 - _A\widetilde{f}(x_i) - _B\widetilde{f}(x_i)\right)\log_{\frac{3}{2}}\left\{\frac{4 - _A\widetilde{f}(x_i) - _B\widetilde{f}(x_i)}{\frac{2}{3}\left[5 - _A\widetilde{f}(x_i) - _B\widetilde{f}(x_i) + \sqrt{\left(1 - _A\widetilde{f}(x_i)\right)\left(1 - _B\widetilde{f}(x_i)\right)}\right]}\right\}\end{array}\right]$$

Proof. It is quite straightforward

3.6 Theorem For any two SVNSs $A, B \in X, \exists$ the inequality $0 \leq _{\text{SVNS}} K(A,B) \leq 18\left(2 - \log_{\frac{3}{2}}2\right)n$, for a fixed n.

Proof. Replacement of B with the complement of A into the resulting **Theorem 3.5** yields

measure to identify faults of some rolling bearing elements installed in a test rig and axial piston pump.

4. Application of the proposed SVNCE measure for identifying defects of bearing installed in customized test rig

$$
\begin{aligned}
_{\text{SVNS}}K\left(A,A^c\right) &= 2\sum_{i=1}^{n}\left[\begin{array}{l}\left(2 +_A \tilde{\mu}(x_i) +_A \tilde{f}(x_i)\right)\log_{\frac{3}{2}}\left[\frac{1}{\frac{2}{3}\left[1+\frac{1+\sqrt{_A\tilde{\mu}(x_i)_A\tilde{f}(x_i)}}{2+_A\tilde{\mu}(x_i)+_A\tilde{f}(x_i)}\right]}\right] + \left(4 -_A \tilde{\mu}(x_i) -_A \tilde{f}(x_i)\right)\times \\[2em] \log_{\frac{3}{2}}\left[\frac{1}{\frac{2}{3}\left[1+\frac{1+\sqrt{\left(1-_A\tilde{\mu}(x_i)\right)\left(1-_A\tilde{f}(x_i)\right)}}{4-_A\tilde{\mu}(x_i)-_A\tilde{f}(x_i)}\right]}\right] + 3\log_{\frac{3}{2}}\left[\frac{3}{\frac{8}{3}\left[1+\frac{1}{4}\sqrt{_A\tilde{i}(x_i)\left(1-_A\tilde{i}(x_i)\right)}\right]}\right]\end{array}\right] \\[3em]
&= 2\sum_{i=1}^{n}\left[\begin{array}{l}6+3\log_{\frac{3}{2}}\frac{9}{8} \\[1em] -\left(\begin{array}{l}\left(2+_A\tilde{\mu}(x_i)+_A\tilde{f}(x_i)\right)\log_{\frac{3}{2}}\left[1+\frac{1+\sqrt{_A\tilde{\mu}(x_i)_A\tilde{f}(x_i)}}{2+_A\tilde{\mu}(x_i)+_A\tilde{f}(x_i)}\right]+\left(4-_A\tilde{\mu}(x_i)-_A\tilde{f}(x_i)\right)\times \\[1em] \log_{\frac{3}{2}}\left[1+\frac{1+\sqrt{\left(1-_A\tilde{\mu}(x_i)\right)\left(1-_A\tilde{f}(x_i)\right)}}{4-_A\tilde{\mu}(x_i)-_A\tilde{f}(x_i)}\right]+3\log_{\frac{3}{2}}\left[1+\frac{1}{4}\sqrt{_A\tilde{i}(x_i)\left(1-_A\tilde{i}(x_i)\right)}\right]\end{array}\right)\end{array}\right] \\[3em]
&= 2\sum_{i=1}^{n}\left[6+3\log_{\frac{3}{2}}\frac{9}{8}+3\left(2-2\log_{\frac{3}{2}}2\right)-3\left(\begin{array}{l}2-2\log_{\frac{3}{2}}2+\frac{\left(2+_A\tilde{\mu}(x_i)+_A\tilde{f}(x_i)\right)}{3}\log_{\frac{3}{2}}\left[1+\frac{1+\sqrt{_A\tilde{\mu}(x_i)_A\tilde{f}(x_i)}}{2+_A\tilde{\mu}(x_i)+_A\tilde{f}(x_i)}\right] \\[1em] +\frac{\left(4-_A\tilde{\mu}(x_i)-_A\tilde{f}(x_i)\right)}{3}\log_{\frac{3}{2}}\left[1+\frac{1+\sqrt{\left(1-_A\tilde{\mu}(x_i)\right)\left(1-_A\tilde{f}(x_i)\right)}}{4-_A\tilde{\mu}(x_i)-_A\tilde{f}(x_i)}\right] \\[1em] +\log_{\frac{3}{2}}\left[1+\frac{1}{4}\sqrt{_A\tilde{i}(x_i)\left(1-_A\tilde{i}(x_i)\right)}\right]\end{array}\right)\right]
\end{aligned}
$$

Plugging the result of **Theorem 3.4** into the foregoing equation, which on reinterpretation, gives

$$
_{\text{SVNS}}K\left(A,A^c\right) = 18\left(2-\log_{\frac{3}{2}}2\right)n - 6_N\tilde{H}(A) \tag{6}
$$

Employment of the non-negative condition: $_N\tilde{H}(A) \geq 0 \forall_A \tilde{\mu}(x_i),_A \tilde{i}(x_i),_A \tilde{f}(x_i) \in [0,1]$ into the resulting equation (6) yields

$$
0 \leq_A \tilde{H}(A) = 3\left(2-\log_{\frac{3}{2}}2\right)n - \frac{1}{6}_{\text{SVNS}}K\left(A,A^c\right) \leq 0 \Rightarrow 0
$$

$$
\leq_{\text{SVNS}} K\left(A,A^c\right) \leq 18\left(2-\log_{\frac{3}{2}}2\right)n \tag{7}
$$

Discussion:-The resulting inequality (7) suggests that $_{\text{SVNS}}K(A,B)$ satisfies the inequality: $0 \leq_{\text{SVNS}} K(A,B) \leq 18\left(2-\log_{\frac{3}{2}}2\right)n$. Since the maximum value of $_N\tilde{H}(A)$ is $3\left(2-\log_{\frac{3}{2}}2\right)n$, equation (**7**) permits us to suggest that the minimum value of $_{\text{SVNS}}K(A,B)$ is zero. Also, when A is a crisp set, then, the minimum value of $_N\tilde{H}(A)$ is zero and hence (7) yields that the maximum value of $_{\text{SVNS}}K(A,B)$ is $18\left(2-\log_{\frac{3}{2}}2\right)n$ for a given n and this value is independent on the elements in X and depends only on the cardinality of the universe of discourse X.

In the following section, we shall, equally well, provide the applicability and feasibility of the newly discovered SVNCE

4.1. Experimental set up

This investigational study was done on a test rig shown in Fig. 4. The two bearings (bearing 1 and bearing 2) at both ends support the shaft. A 346-watt AC motor gives power to the shaft via pulley arrangement. A disc of mass 2 Kg is attached in the middle of the shaft (between bearing 1 and bearing 2) which rotates along with the shaft. The bearing is loaded in the vertical direction through a lever arrangement. For the measurement of applied load, the test rig also has a load cell beneath the bearing housing. The shaft speed can be measured by a proximity sensor. Vibrations signal from the test rig were measured by mounting accelerometer on the bearing housing. The bearing used for analysis is cylindrical roller bearing ((NBC: NU205E)) with specifications given in Table 2. The photograph of defective components of bearing is shown in Fig. 5. A seeded groove of defect width 0.5 mm was generated on the outer and inner race of the bearing.

4.2. Vibrational signal data processing

The framework of the proposed methodology for identifying faults in some rolling bearing is shown in Fig. 6. In this study, vibration signals under the conditions-(a) fault free, (b) bearing with faults on outer race and (c) bearing with faults on inner race – were acquired. The data acquisition device NI-USB-4431 was used to acquire vibration data. Typical raw vibration signals under the three mentioned conditions are shown in Fig. 7(a–c). The recorded
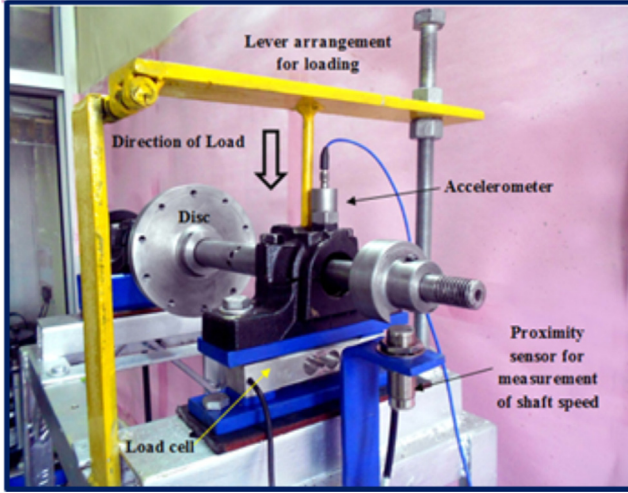
Fig. 4. A Typical view of the test rig.

Table 2
Specification of the cylindrical rolling bearing installed in customized test rig.

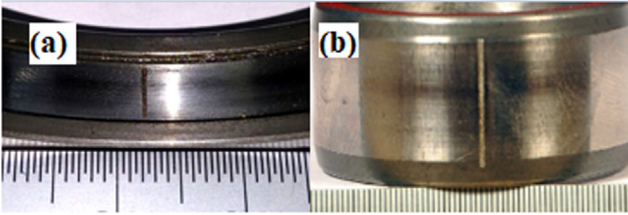| Pitch Diameter (D)	38.9 mm
Ball Diameter (d)	7.5 mm
Number of rolling elements (N)	13
Contact angle (φ)	0°

Fig. 5. Photograph of defective components of cylindrical rolling bearing (a) Outer race (b) Inner race.

signals were processed in MATLAB environment and all the acquired signals were decomposed by applying 3-level WPT with Symlet 2 wavelet. A total of 270 signals were acquired, 90 under each condition. Out of which, 30 signals under each condition, were used to develop the model and the remaining 60 signals to test the model.

4.3. Wavelet packet decomposition

Let k represents the number of sub-frequency bands and $y_{3,k}(t)$ denotes the wavelet coefficient at 3-level and k^{th} sub frequency band. Let $y(t)$ be any particular vibration signal, then $y(t) = \sum_{k=0}^{2^3-1} y_{3,k}(t)$. A 3-level wavelet packet decomposition concentrates the vibration signals generated by faulty bearings into $2^3 - 1 = 8$ sub-frequency bands. The sub-frequency bands at 3-level of decomposition for fault-free, bearing with faults on its outer race and inner race respectively are shown in Figs. 8–10 respectively. The sampling frequency in this work is $f_s = 70,000$ samples per sec. The frequency intervals of each band can be calculated by using the formula $\left[\frac{(k-1)f_s}{2^4}, \frac{kf_s}{2^4}\right]$.

The eight sub-frequency bands corresponding to the various signals $y_{3,i}(i = 0, 1, 2, ...7)$ are: $(0, 4375], (4375, 8750], (8750,$
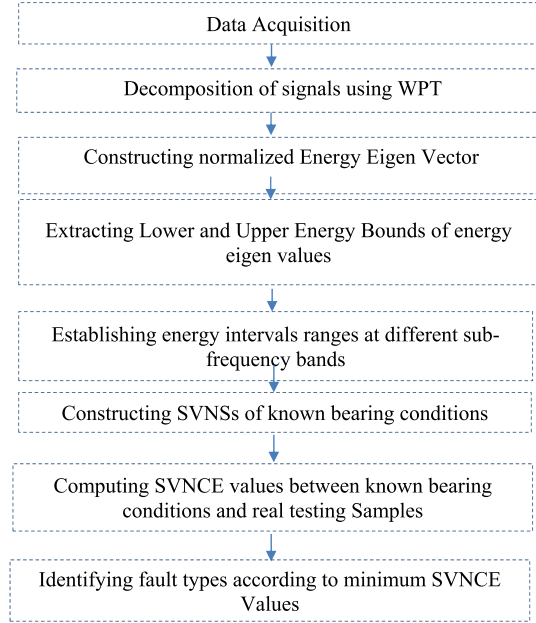

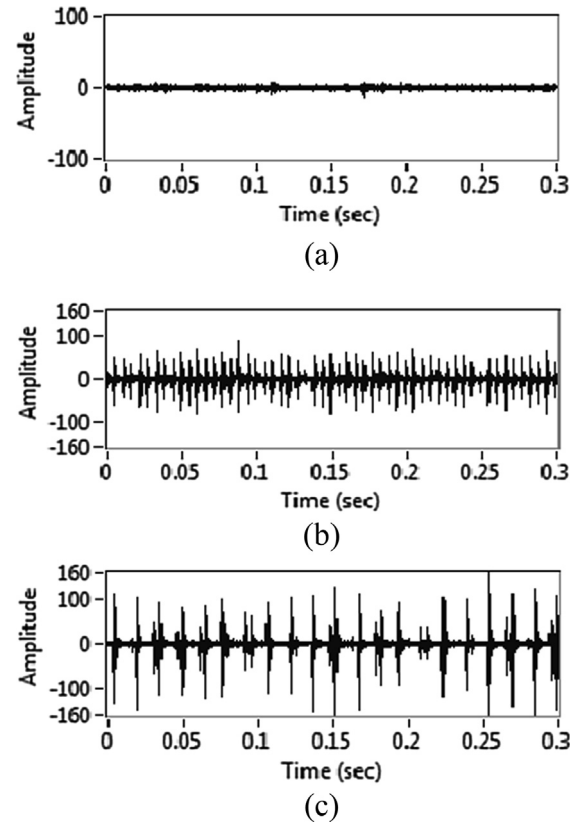**Fig. 6.** Block diagram for identifying bearing faults using the proposed SVNCE measure.

Fig. 7. Raw vibration signals under different conditions (a) fault-free (b) bearing with faults on outer race and (c) bearing with faults on the inner race.

$13125], (13125, 17500], (17500, 21875], (21875, 26250] (26250, 30625], (30625, 35000]$

Let, after decomposition, P_3^k represents the energy eigenvector of the kth sub frequency band and $y_{3,k}(i)$ is the ith discrete point amplitude of the wavelet coefficient $y_{3,k}(t)$, then
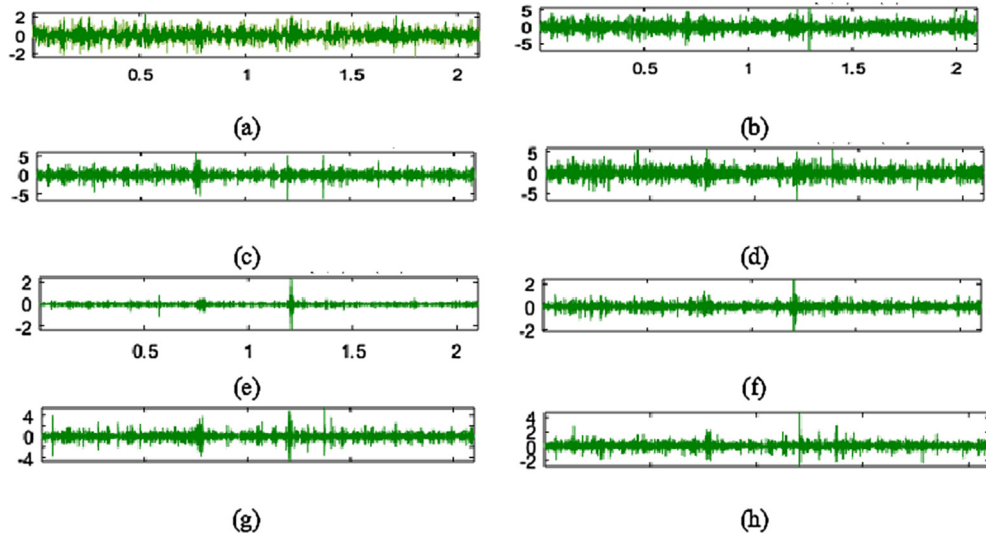
Fig. 8. Sub-frequency bands under fault free condition: $(a)\,y_{3,7}\,(b)\,y_{3,6}\,(c)\,y_{3,5}\,(d)\,y_{3,4}\,(e)\,y_{3,3}\,(f)\,y_{3,2}\,(g)\,y_{3,1}\,(h)\,y_{3,0}$.
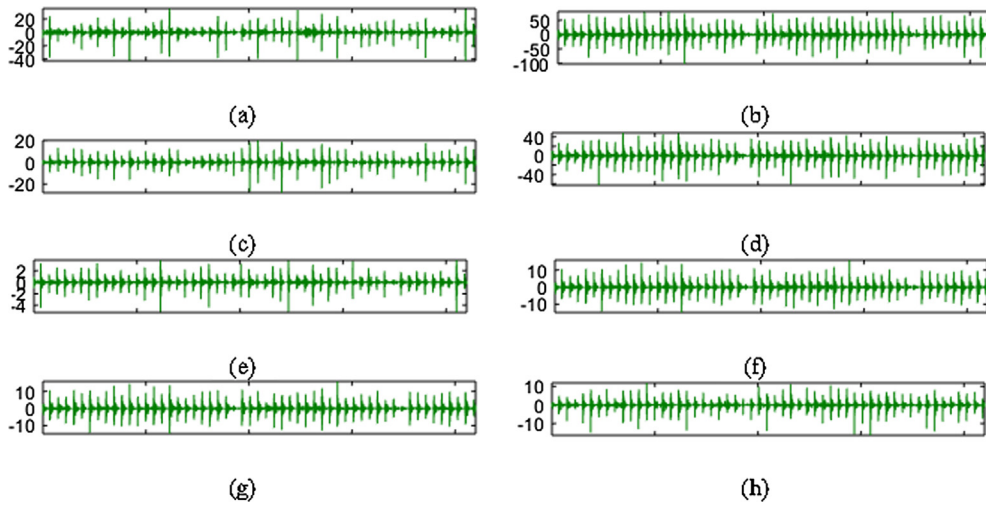
Fig. 9. Sub-frequency bands under outer race fault condition $(a)\,y_{3,7}\,(b)\,y_{3,6}\,(c)\,y_{3,5}\,(d)\,y_{3,4}\,(e)\,y_{3,3}\,(f)\,y_{3,2}\,(g)\,y_{3,1}\,(h)\,y_{3,0}$.
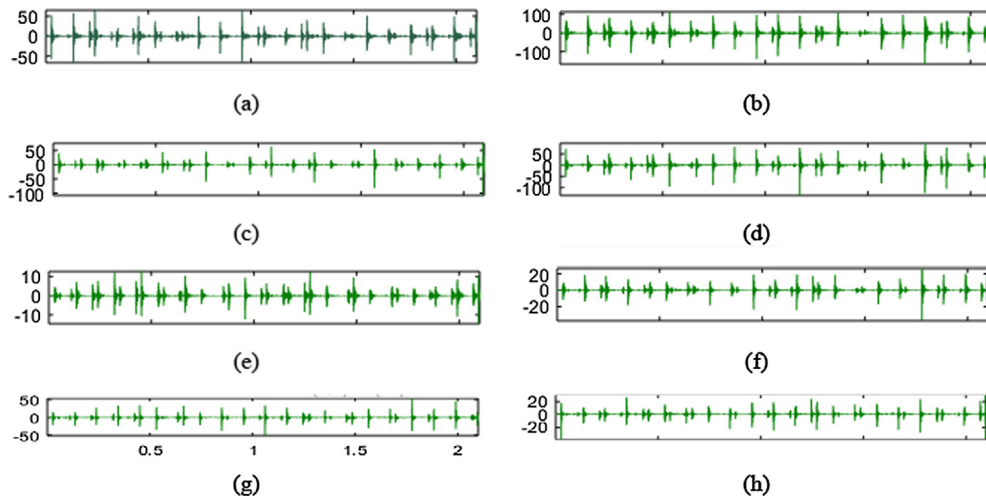
Fig. 10. Sub-frequency band under inner race fault condition: $(a)\,y_{3,7}\,(b)\,y_{3,6}\,(c)\,y_{3,5}\,(d)\,y_{3,4}\,(e)\,y_{3,3}\,(f)\,y_{3,2}\,(g)\,y_{3,1}\,(h)\,y_{3,0}$.

$P_3^k = \sum_{i=0}^{2^3-1} |y_{3,k}(t)|^2; k = 0, 1, \ldots 7$. The wavelet packet energy is greatly influenced with the faults of rolling bearings, so it becomes necessary to extract the energy eigenvalue for diagnosing faults of rolling bearings.

$$Let\ T = \left[P_3^0, P_3^1, P_3^2, P_3^3, P_3^4, P_3^5, P_3^6, P_3^7 \right] \tag{8}$$

then T is called as energy eigenvector and can be constructed based on energy eigenvalues of each sub-frequency bands. Let Max.P_3 and Min.P_3 represents the maximum and minimum energy eigen value in a 3-level sub-frequency band respectively. For diagnosing faults of rolling bearings, it is necessary to normalize these energy eigenvalues of the wavelet packet energy to be bounded in the interval [0,1]. Thus, the normalized energy eigenvector T can be described as:

$$T^* = \left[P_3^{*0}, P_3^{*1}, P_3^{*2}, P_3^{*3}, P_3^{*4}, P_3^{*5}, P_3^{*6}, P_3^{*7} \right];$$
$$where\ P_3^{*k} = \frac{P_3^k - Min.P_3^k}{Max.P_3^k - Min.P_3^k}; k = 0, 1, 2, \ldots 7. \tag{9}$$

The normalized energy eigenvalues of vibration signals are represented in the Energy Histograms displayed in Fig. 11. For different types of faulty bearing, the eigenvalue of the wavelet packet energy has the distinguishing distribution at the individual sub frequency band. Based upon a lot of experimentation and data comparison, we have been able to extract lower and upper bounds of the normalized energy eigen value for each knowledge of fault types and establish the energy interval ranges as represented in Table 3. In the present case, we represent the knowledge of fault types experienced by rolling bearing by the set $A = (A_1, A_2, A_3)$ where A_1 = Fault free bearing, A_2 = Bearing with fault on its outer race and A_3 = Bearing with fault on its inner race. This research paper considers equal importance of each energy eigen value in each sub-frequency band, therefore, the weights can be assumed as $w_i = \frac{1}{8} (i = 1, 2, \ldots 8)$.

4.4. Identification of faults of rolling bearing installed in a customized test rig

Let $\tilde{\mu}_{A_K}(x_i)$ and $\tilde{U}_{A_K}(x_i)(K = 1, 2, 3; i = 1, 2, \ldots, 8)$ represent the lower and upper bounds of the ith energy eigen value for a typical knowledge of fault type $A_K(K = 1, 2, 3)$. Then, the energy interval ranges for typical faults types can be represented as:
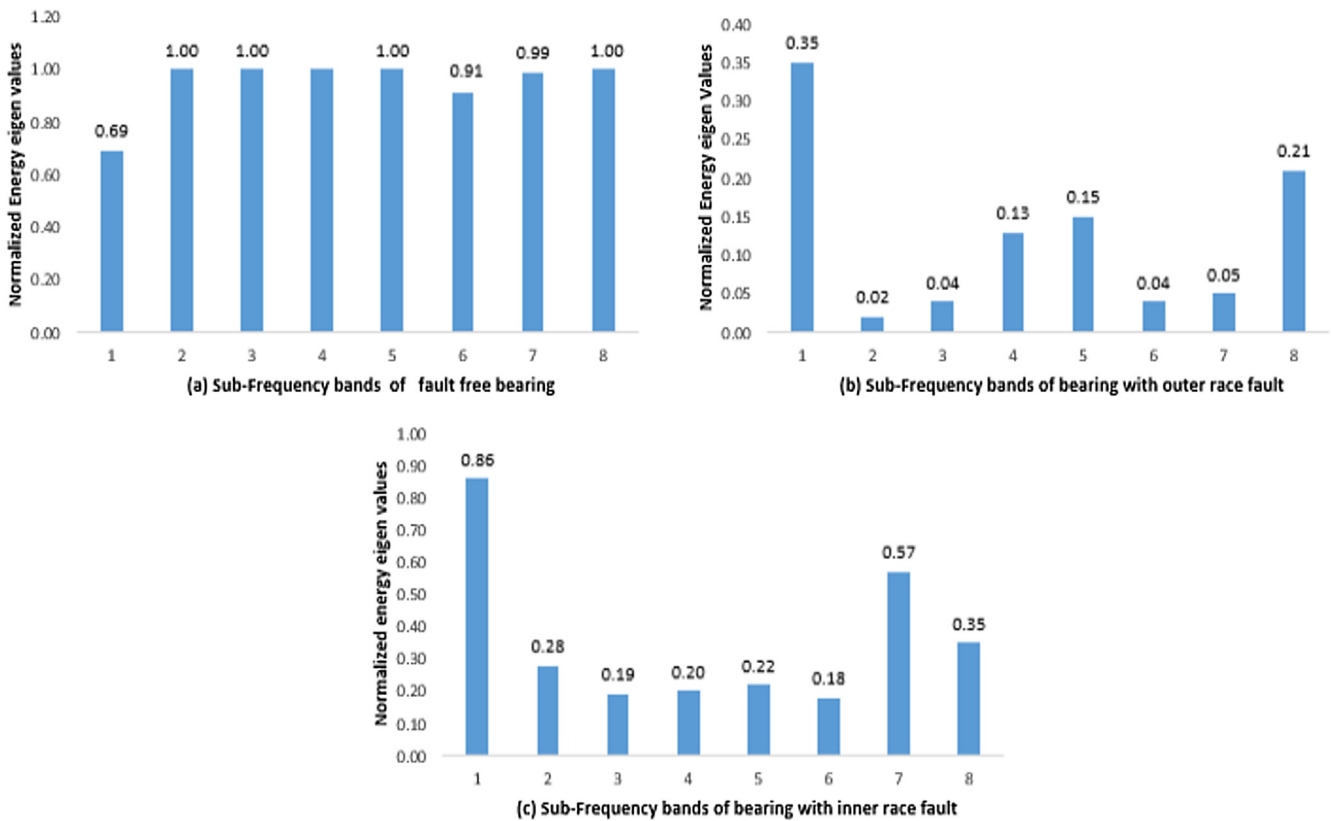

Fig. 11. Energy Histograms of (a) Fault free bearing (b) bearing with fault on its outer race (c) bearing with fault on its inner race.

Table 3
Energy interval ranges of eight sub-frequency bands.

Fault Types	Energy in each sub-frequency band							
	P_3^{*0}	P_3^{*1}	P_3^{*2}	P_3^{*3}	P_3^{*4}	P_3^{*5}	P_3^{*6}	P_3^{*7}
A_1: Fault-Free	[0.31 0.69]	[0.54 1.00]	[0.31 1.00]	[0.40 1.00]	[0.48 1.00]	[0.21 0.91]	[0.38 0.99]	[0.36 1.00]
A_2: Inner race	[0.00 0.35]	[0.01 0.02]	[0.02 0.04]	[0.02 0.13]	[0.05 0.10]	[0.01 0.04]	[0.00 0.05]	[0.01 0.21]
A_3: Outer race	[0.05 0.86]	[0.00 0.28]	[0.00 0.19]	[0.01 0.20]	[0.00 0.22]	[0.00 0.18]	[0.13 0.57]	[0.06 0.35]

$$A_K = \begin{cases} < x_1, \left[\tilde{\mu}_{A_K}(x_1), \tilde{U}_{A_K}(x_1)\right] >, < x_2, \left[\tilde{\mu}_{A_K}(x_2), \tilde{U}_{A_K}(x_2)\right] >, < x_3, \left[\tilde{\mu}_{A_K}(x_3), \tilde{U}_{A_K}(x_3)\right] >, \\ < x_4, \left[\tilde{\mu}_{A_K}(x_4), \tilde{U}_{A_K}(x_4)\right] >, < x_5, \left[\tilde{\mu}_{A_K}(x_5), \tilde{U}_{A_K}(x_5)\right] >, < x_6, \left[\tilde{\mu}_{A_K}(x_6), \tilde{U}_{A_K}(x_6)\right] >, \\ < x_7, \left[\tilde{\mu}_{A_K}(x_7), \tilde{U}_{A_K}(x_7)\right] >, < x_8, \left[\tilde{\mu}_{A_K}(x_8), \tilde{U}_{A_K}(x_8)\right] > \end{cases}$$

Table 4
Energy interval ranges of typical fault types at eight sub-frequency band represented in the form of SVNSs.

| Fault Types | Energy in each frequency Band | | | | | | | |
	P_3^{*0}	P_3^{*1}	P_3^{*2}	P_3^{*3}	P_3^{*4}	P_3^{*5}	P_3^{*6}	P_3^{*7}
A_1	[0.31 0.38 0.31]	[0.54 0.4 0.00]	[0.31 0.69 0.00]	[0.40 0.60 0.00]	[0.48 0.52 0.00]	[0.21 0.70 0.09]	[0.38 0.61 0.01]	[0.36 0.64 0.00]
A_2	[0.00 0.35 0.65]	[0.01 0.01 0.98]	[0.02 0.02 0.96]	[0.02 0.11 0.87]	[0.05 0.10 0.85]	[0.01 0.03 0.96]	[0.00 0.05 0.95]	[0.01 0.01 0.79]
A_3	[0.05 0.81 0.14]	[0.00 0.28 0.72]	[0.00 0.19 0.81]	[0.01 0.19 0.80]	[0.00 0.22 0.78]	[0.00 0.18 0.82]	[0.13 0.44 0.43]	[0.06 0.29 0.65]

Let $\tilde{f}_{A_K}(x_i) = 1 - \tilde{U}_{A_K}(x_i)$ and $\tilde{i}_{A_K}(x_i) = 1 - \tilde{f}_{A_K}(x_i) - \tilde{U}_{A_K}(x_i)$ where the values of $\tilde{i}_{A_K}(x_i)$ is restricted to $0 \cdot 01$ if it is less than $0 \cdot 001$. Then, the set A_K can be extended to SVNSs as shown in Table 4 and re-written as:

$$A_K = \begin{cases} < x_1, \left[\tilde{\mu}_{A_K}(x_1), \tilde{i}_{A_K}(x_1), \tilde{f}_{A_K}(x_1)\right] >, < x_2, \left[\tilde{\mu}_{A_K}(x_2), \tilde{i}_{A_K}(x_2), \tilde{f}_{A_K}(x_2)\right] >, \\ < x_3, \left[\tilde{\mu}_{A_K}(x_3), \tilde{i}_{A_K}(x_3), \tilde{f}_{A_K}(x_3)\right] >, < x_4, \left[\tilde{\mu}_{A_K}(x_4), \tilde{i}_{A_K}(x_4), \tilde{f}_{A_K}(x_4)\right] >, \\ < x_5, \left[\tilde{\mu}_{A_K}(x_5), \tilde{i}_{A_K}(x_5), \tilde{f}_{A_K}(x_5)\right] >, < x_6, \left[\tilde{\mu}_{A_K}(x_6), \tilde{i}_{A_K}(x_6), \tilde{f}_{A_K}(x_6)\right] >, \\ < x_7, \left[\tilde{\mu}_{A_K}(x_7), \tilde{i}_{A_K}(x_7), \tilde{f}_{A_K}(x_7)\right] >, < x_8, \left[\tilde{\mu}_{A_K}(x_8), \tilde{i}_{A_K}(x_8), \tilde{f}_{A_K}(x_8)\right] > \end{cases};$$

satisfying $\mu_{A_K}(x_1), i_{A_K}(x_1), f_{A_K}(x_1) : X \to [0,1]; \mu_{A_K}(x_1) + i_{A_K}(x_1) + f_{A_K}(x_1) \le 3$

Let the real testing samples $F_{T_j}(j = 1, 2, 3)$ can also be described in the form of SVNSs as:

$$F_{T_1} = \begin{cases} < x_1, [0 \cdot 56, 0 \cdot 32, 0 \cdot 12] >, < x_2, [0 \cdot 60, 0 \cdot 16, 0 \cdot 24] >, < x_3, [0 \cdot 54, 0 \cdot 34, 0 \cdot 12] >, \\ < x_4, [0 \cdot 54, 0 \cdot 32, 0 \cdot 14] >, < x_5, [0 \cdot 46, 0 \cdot 16, 0 \cdot 38] >, < x_6, [0 \cdot 59, 0 \cdot 41, 0 \cdot 00] >, \\ < x_7, [0 \cdot 69, 0 \cdot 31, 0 \cdot 00] >, < x_8, [0 \cdot 70, 0 \cdot 24, 0 \cdot 06] > \end{cases}$$

$$F_{T_2} = \begin{cases} < x_1, [0 \cdot 33, 0 \cdot 09, 0 \cdot 58] >, < x_2, [0 \cdot 03, 0 \cdot 02, 0 \cdot 95] >, < x_3, [0 \cdot 03, 0 \cdot 03, 0 \cdot 94] >, \\ < x_4, [0 \cdot 00, 0 \cdot 03, 0 \cdot 97] >, < x_5, [0 \cdot 05, 0 \cdot 03, 0 \cdot 92] >, < x_6, [0 \cdot 04, 0 \cdot 03, 0 \cdot 93] >, \\ < x_7, [0 \cdot 03, 0 \cdot 02, 0 \cdot 95] >, < x_8, [0 \cdot 10, 0 \cdot 06, 0 \cdot 84] > \end{cases}$$

$$F_{T_3} = \begin{cases} < x_1, [0 \cdot 75, 0 \cdot 25, 0 \cdot 00] >, < x_2, [0 \cdot 26, 0 \cdot 07, 0 \cdot 67] >, < x_3, [0 \cdot 04, 0 \cdot 04, 0 \cdot 92] >, \\ < x_4, [0 \cdot 01, 0 \cdot 04, 0 \cdot 95] >, < x_5, [0 \cdot 15, 0 \cdot 08, 0 \cdot 77] >, < x_6, [0 \cdot 17, 0 \cdot 05, 0 \cdot 78] >, \\ < x_7, [0 \cdot 58, 0 \cdot 34, 0 \cdot 08] >, < x_8, [0 \cdot 36, 0 \cdot 28, 0 \cdot 36] > \end{cases}$$

In short, the defined values of real testing samples can be finally represented into the form of SVNSs as

$$F_{T_j}(j = 1, 2, 3) = \left\{ < x_i, \left[\tilde{\mu}_{F_{T_j}}(x_i), \tilde{i}_{F_{T_j}}(x_i), \tilde{f}_{F_{T_j}}(x_i)\right] > \right\}; (i = 1, 2, 3, .., 8).$$

With due permission of the resulting SVNSs and replacing $_A\tilde{\mu}(x), _A\tilde{i}(x), _A\tilde{f}(x)$ with newly defined $\tilde{\mu}_{A_K}(x), \tilde{i}_{A_K}(x), \tilde{f}_{A_K}(x)$ respectively, the newly discovered SVNCE measure in **Theorem 3.5** takes the following form:

$$_{SVNS}K\left(A_K, F_{T_j}\right)(K = 1, 2, 3 : j = 1, 2, 3)$$

$$= \sum_{i=1}^{8} w_i \left[\left(2 + \tilde{\mu}_{A_K}(x_i) + \tilde{\mu}_{F_{T_j}}(x_i)\right) \log_{\frac{3}{2}} \left[\frac{2 + \tilde{\mu}_{A_K}(x_i) + \tilde{\mu}_{F_{T_j}}(x_i)}{\frac{2}{3}\left[3 + \tilde{\mu}_{A_K}(x_i) + \tilde{\mu}_{F_{T_j}}(x_i) + \sqrt{\tilde{\mu}_{A_K}(x_i)\tilde{\mu}_{F_{T_j}}(x_i)}\right]} \right] + \left(4 - \tilde{\mu}_{A_K}(x_i) - \tilde{\mu}_{F_{T_j}}(x_i)\right) \log_{\frac{3}{2}} \left[\frac{4 - \tilde{\mu}_{A_K}(x_i) - \tilde{\mu}_{F_{T_j}}(x_i)}{\frac{2}{3}\left[5 - \tilde{\mu}_{A_K}(x_i) - \tilde{\mu}_{F_{T_j}}(x_i) + \sqrt{\left(1 - \tilde{\mu}_{A_K}(x_i)\right)\left(1 - \tilde{\mu}_{F_{T_j}}(x_i)\right)}\right]} \right] \right]$$

$$+ \sum_{i=1}^{8} w_i \left[\left(2 + \tilde{i}_{A_K}(x_i) + \tilde{i}_{F_{T_j}}(x_i)\right) \log_{\frac{3}{2}} \left[\frac{2 + \tilde{i}_{A_K}(x_i) + \tilde{i}_{F_{T_j}}(x_i)}{\frac{2}{3}\left[3 + \tilde{i}_{A_K}(x_i) + \tilde{i}_{F_{T_j}}(x_i) + \sqrt{\tilde{i}_{A_K}(x_i)\tilde{i}_{F_{T_j}}(x_i)}\right]} \right] + \left(4 - \tilde{i}_{A_K}(x_i) - \tilde{i}_{F_{T_j}}(x_i)\right) \log_{\frac{3}{2}} \left[\frac{4 - \tilde{i}_{A_K}(x_i) - \tilde{i}_{F_{T_j}}(x_i)}{\frac{2}{3}\left[5 - \tilde{i}_{A_K}(x_i) - \tilde{i}_{F_{T_j}}(x_i) + \sqrt{\left(1 - \tilde{i}_{A_K}(x_i)\right)\left(1 - \tilde{i}_{F_{T_j}}(x_i)\right)}\right]} \right] \right]$$

$$+ \sum_{i=1}^{8} w_i \left[\left(2 + \tilde{f}_{A_K}(x_i) + \tilde{f}_{F_{T_j}}(x_i)\right) \log_{\frac{3}{2}} \left[\frac{2 + \tilde{f}_{A_K}(x_i) + \tilde{f}_{F_{T_j}}(x_i)}{\frac{2}{3}\left[3 + \tilde{f}_{A_K}(x_i) + \tilde{f}_{F_{T_j}}(x_i) + \sqrt{\tilde{f}_{A_K}(x_i)\tilde{f}_{F_{T_j}}(x_i)}\right]} \right] + \left(4 - \tilde{f}_{A_K}(x_i) - \tilde{f}_{F_{T_j}}(x_i)\right) \log_{\frac{3}{2}} \left[\frac{4 - \tilde{f}_{A_K}(x_i) - \tilde{f}_{F_{T_j}}(x_i)}{\frac{2}{3}\left[5 - \tilde{f}_{A_K}(x_i) - \tilde{f}_{F_{T_j}}(x_i) + \sqrt{\left(1 - \tilde{f}_{A_K}(x_i)\right)\left(1 - \tilde{f}_{F_{T_j}}(x_i)\right)}\right]} \right] \right]$$

$$(10)$$

The SVNCE values $_{SVNS}K\left(A_K, F_{T_j}\right)$ between real testing samples $F_{T_j}(j = 1, 2, 3)$ and various knowledge of fault types $A_K(K = 1, 2, 3)$ can be calculated using Eq. (10). Using Minimum argument principle of fault diagnosis, the fault diagnosis order and fault condition type of all three kinds of bearings obtained by the proposed SVNCE measure as well as by the existing method [21] are represented below (Table 5).

4.5. Diagnosis results and comparative analysis

The diagnosis can be carried out by computing minimum SVNCE values between the real testing samples $F_{T_j}(j = 1, 2, 3)$ and various

Table 5
Fault diagnosis order obtained by the proposed method and the existing method based on SNSs [21].

Existing method based upon SNSs						
Measure	Correlation coefficient Values			Fault diagnosis order	Fault condition identified	Actual fault condition
	A_1	A_2	A_3			
$M_{SNS}(A_K, F_{T_1})$	0.7551	0.4109	0.5909	$A_1 \rightarrow A_2 \rightarrow A_3$	Healthy	Healthy
$M_{SNS}(A_K, F_{T_2})$	0.3117	0.9432	0.7655	$A_2 \rightarrow A_3 \rightarrow A_1$	Outer race	Outer race
$M_{SNS}(A_K, F_{T_3})$	0.5389	0.7703	0.8063	$A_3 \rightarrow A_2 \rightarrow A_1$	Inner Race	Inner Race
Proposed method based upon SVNSs						
Measure	SVNCE Values			Fault diagnosis order	Fault condition identified	Actual fault condition
	A_1	A_2	A_3			
$_{SVNS}K(A_K, F_{T_1})$	0.2606	1.2923	0.8627	$A_1 \rightarrow A_3 \rightarrow A_2$	Healthy	Healthy
$_{SVNS}K(A_K, F_{T_2}))$	1.5942	0.0770	0.2618	$A_2 \rightarrow A_3 \rightarrow A_1$	Outer race	Outer race
$_{SVNS}K(A_K, F_{T_3})$	1.0026	0.5197	0.2689	$A_3 \rightarrow A_2 \rightarrow A_1$	Inner Race	Inner Race

Table 6
Confusion matrix showing classification performance on test data using the proposed method based on SVNSs.

		Predicted Class			Overall accuracy %
		Fault free	Fault on Outer race	Fault on Inner race	
Actual Class	Fault free	60	0	0	100
	Fault on outer race	0	60	0	
	Fault on inner Race fault	0	0	60	

Table 7
Fault identification accuracy of the proposed method and the existing method based on SNSs.

Method	Accuracy %			Overall accuracy %
	Fault free	Outer race fault	Inner race fault	
Existing method based on SNSs [25] method	100	100	93.3	97.7
Proposed method based on SVNSs method	100	100	100	100

knowledge of fault types $A_K(K = 1, 2, 3)$ as shown in Table 5**.** The results of Table 5 provide us the information that the proposed SVNCE measure $_{SVNCE}K(A_K, F_{T_j})(j = 1, 2, 3)$ returns exactly the same fault diagnosis order and fault condition type as returned by the existing method [21].

Diagnosis result 1. The minimum SVNCE value between the first real testing sample F_{T_1} and $A_K(K = 1, 2, 3)$ is 0.2606,which corresponds to the condition type A_1, i.e., healthy condition. Similarly, the maximum value of $M_{SNS}(A_K, F_{T_1})$ is 0.7551 which corresponds to the condition type A_1. On inspection, it was discovered that bearing was healthy.

Diagnosis result 2. For the second real testing sample F_{T_2}, the minimum value of $_{SVNS}K(A_K, F_{T_2})$ is 0.0770 which corresponds to the condition type A_2 which indicates that the fault is first resulted from the damage of outer race. Similarly, the maximum value of $M_{SNS}(A_K, F_{T_2})$ is 0.9432, which corresponds to the condition type A_2. Furthermore, on inspection of bearing, it was found that bearing was damaged, and it was having defect on its outer race.

Diagnosis result 3. For the third real testing sample F_{T_3}, the minimum value of $_{SVNS}K(A_K, F_{T_3})$ is 0.2689 which corresponds to the main fault type A_3 which indicates that the fault is resulted from the damage of inner race. Similarly, the maximum value of $M_{SNS}(A_K, F_{T_3})$ is 0.8063, which corresponds to the condition type A_3. Also, during checking of bearing, we discover that the bearing was damaged, and it was having defect on its inner race. The above discussion validates the effectiveness and reliability of the proposed SVNCE measure based upon SVNSs.

4.6. Fault identification accuracy of the proposed SVNCE measure
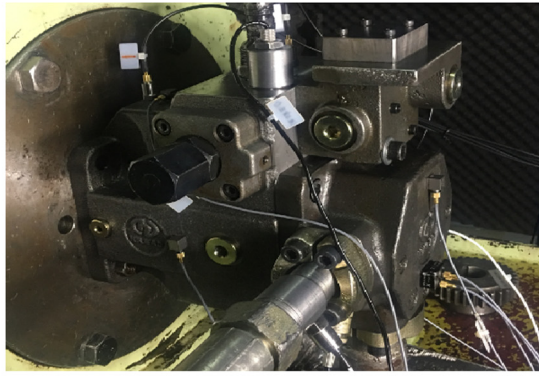
The fault identification accuracy of the proposed method based upon SVNSs is 100% (Table 6) and is also compared with the existing method based on SNSs [21]. The comparison is presented in Table 7 which verifies that the fault identification accuracy of the proposed method is much better than the well-established prediction method based on SNSs.

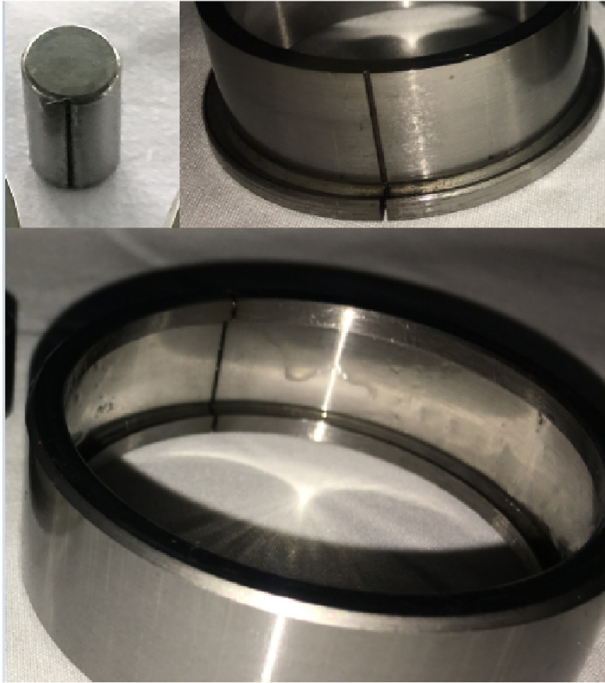### 5. Application of the proposed SVNCE measure to identify bearing defects of axial pump

In this section, we shall apply the proposed method to identify bearing defects of axial pump. The experiments were performed on the customized test rig as shown in Fig. 12(a). The test rig was manufactured by Ningbo Hilead Hydraulic Co., Ltd. and is equipped with speed monitor, manual speed and pressure governor, accelerometer, serve motor, data acquisition device. To simulate the defect conditions, damage was produced on the following components mentioned in Table 8. The specification of components of roller bearing under study are given in Table 9. The photograph of defective components is shown in Fig. 12(b).

5.1. Vibrational signal data processing

In this case, vibration signals were acquired under three conditions-(a) bearing with defects on its roller, (b) bearing with defects on its outer race and (c) bearing with defects on its inner
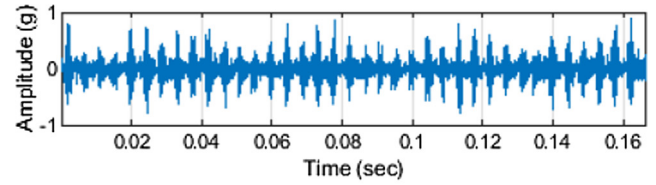
(a)

(b)

(c)

(d)

Fig. 13. Raw vibration signals under different conditions (a) Defect free (b) Bearing with faults on its roller (c) Bearing with faults on its inner race (d) Bearing with faults on its outer race.

race. The signals were processed using the methodology given in Fig. 6. Typical raw vibration signals under the three mentioned conditions are shown in Fig. 13(a–d).

The sub-frequency bands at 3-level of wavelet packet decomposition for bearing with normal condition, faults on its roller, outer race and inner race respectively are shown in Figs. 14–17 respectively. The sampling frequency in this case is 48,000 samples per sec. The frequency intervals of each band can be calculated by using the formula $\left[\frac{(k-1)f_s}{2^4}, \frac{kf_s}{2^4}\right]$, where k represents the number of sub-frequency bands.

The eight sub-frequency bands corresponding to the various signals $y_{3,i}(i = 0, 1, 2, ...7)$ are having frequency:

(0 3000], (3000 6000] (6000 9000] (9000 12000] (12000 15000] (1500 18000] (18000 2100], (18000 24000]. The normalized energy eigenvalues of vibration signals in the present case are represented by the Energy Histograms as displayed in Fig. 18. For different types of knowledge of fault types, the eigen value of the wavelet packet energy has the distinguishing distribution at the individual sub frequency band. Based upon a lot of experimentation and data comparison, we have been able to extract lower and upper bounds of the normalized energy eigen value for each knowledge of fault types and establish the energy interval ranges as represented in Table 10. In this case, we represent the knowledge of fault types experienced by rolling bearing by the set $A = (A_4, A_5, A_6, A_7)$ where A_4 = Bearing with defect free condition, A_5 = Bearing with fault on its roller, A_6= Bearing with fault on its outer race and A_7 = Bearing

(a)

(b)

Fig. 12. (a). Typical view of the test rig and (b) A typical view of the defective components of bearing under study.

Table 8
Defects under study.

Component	Defect type	Size
Bearing	Groove on inner race	0.5 mm
	Groove on outer race	
	Groove on the roller	

Table 9
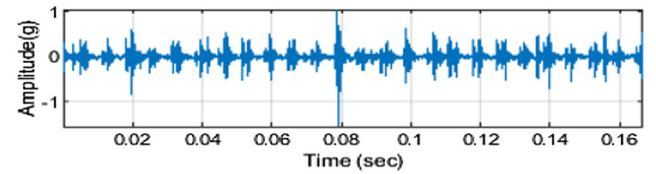Specifications of the cylindrical rollier bearing under study.

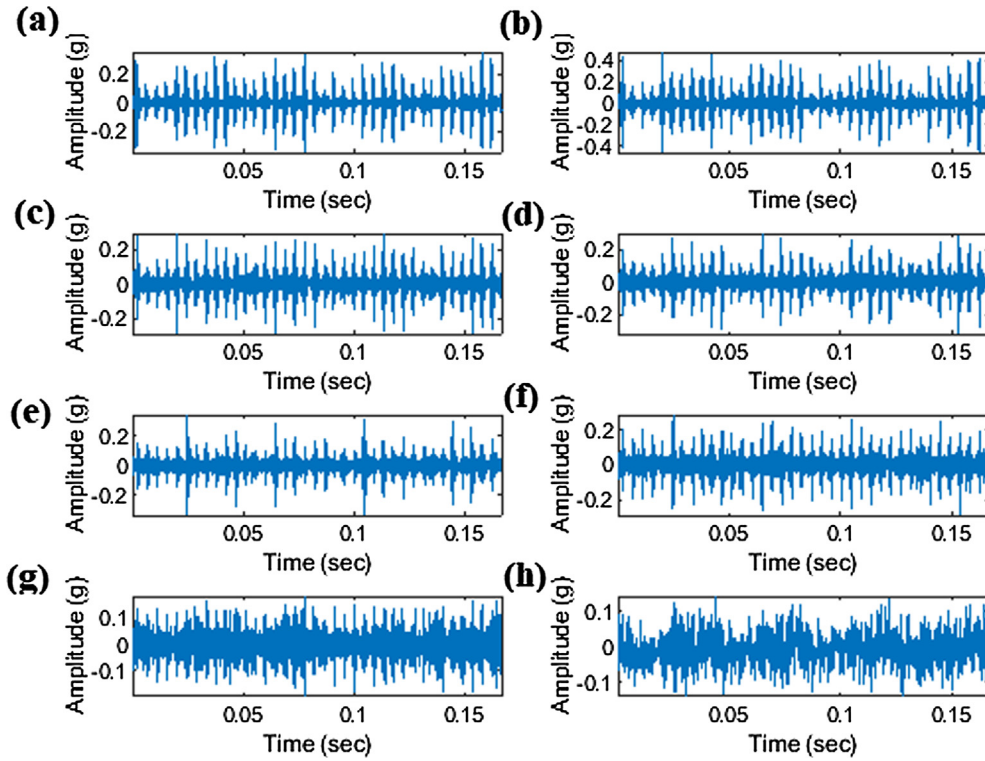|	
Pitch Diameter (D)	49.1 mm
Roller Diameter (d)	9 mm
Number of rolling elements (N)	17
Contact angle (φ)	0°

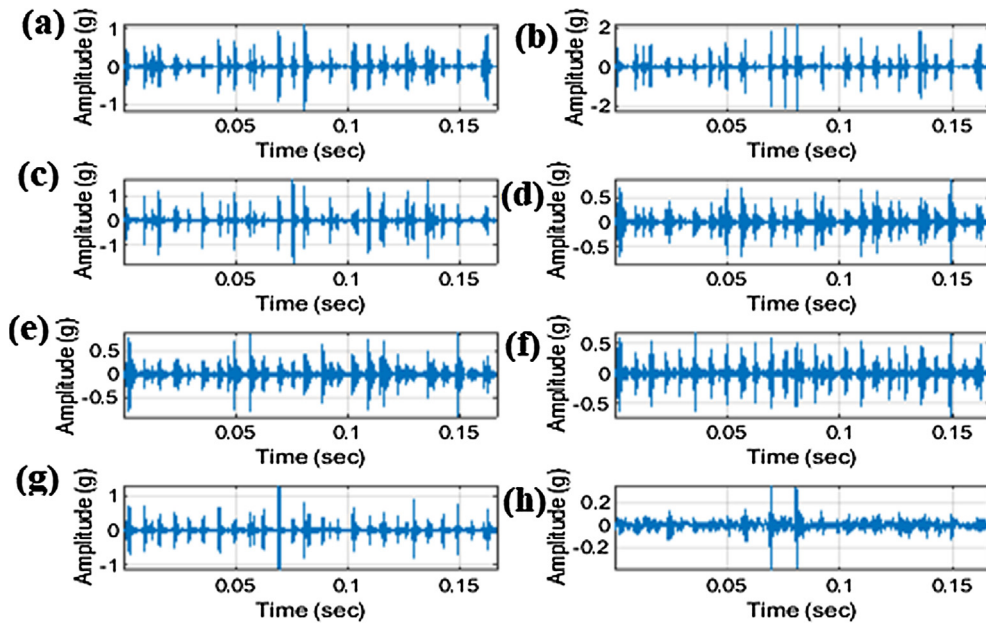**Fig. 14.** Sub-frequency bands under defect free condition.

Fig. 15. Sub-frequency bands under rolling element defect condition: $(a) y_{3,7} (b) y_{3,6} (c) y_{3,5} (d) y_{3,4} (e) y_{3,3} (f) y_{3,2} (g) y_{3,1} (h) y_{3,0}$.

with fault on its inner race. Also, the set $A_K (K = 4, 5, 6, 7)$ can be extended to SVNSs as shown in Table 11.

The real testing samples $F_{T_j} (j = 4, 5, 6, 7)$, can also be described in the form of SVNSs as:

$$F_{T_4} = \left\{ \begin{array}{c} < x_1, [0 \cdot 76, 0 \cdot 14, 0 \cdot 10] >, < x_2, [0 \cdot 09, 0 \cdot 01, 0 \cdot 90] >, < x_3, [0 \cdot 11, 0 \cdot 08, 0 \cdot 81] >, \\ < x_4, [0 \cdot 05, 0 \cdot 04, 0 \cdot 91] >, < x_5, [0 \cdot 05, 0 \cdot 05, 0 \cdot 90] >, < x_6, [0 \cdot 04, 0 \cdot 01, 0 \cdot 95] >, \\ < x_7, [0 \cdot 07, 0 \cdot 06, 0 \cdot 87] >, < x_8, [0 \cdot 10, 0 \cdot 10, 0 \cdot 80] > \end{array} \right\}$$

$$F_{T_5} = \left\{ \begin{array}{c} < x_1, [0 \cdot 57, 0 \cdot 06, 0 \cdot 37] >, < x_2, [0 \cdot 31, 0 \cdot 14, 0 \cdot 55] >, < x_3, [0 \cdot 64, 0 \cdot 05, 0 \cdot 31] >, \\ < x_4, [0 \cdot 34, 0 \cdot 09, 0 \cdot 57] >, < x_5, [0 \cdot 31, 0 \cdot 11, 0 \cdot 58] >, < x_6, [0 \cdot 28, 0 \cdot 13, 0 \cdot 59] >, \\ < x_7, [0 \cdot 11, 0 \cdot 16, 0 \cdot 73] >, < x_8, [0 \cdot 02, 0 \cdot 16, 0 \cdot 82] > \end{array} \right\}$$

$$F_{T_6} = \left\{ \begin{array}{c} < x_1, [0 \cdot 01, 0 \cdot 00, 0 \cdot 99] >, < x_2, [0 \cdot 01, 0 \cdot 00, 0 \cdot 99] >, < x_3, [0 \cdot 07, 0 \cdot 00, 0 \cdot 93] >, \\ < x_4, [0 \cdot 15, 0 \cdot 02, 0 \cdot 83] >, < x_5, [0 \cdot 14, 0 \cdot 01, 0 \cdot 85] >, < x_6, [0 \cdot 02, 0 \cdot 00, 0 \cdot 98] >, \\ < x_7, [0 \cdot 01, 0 \cdot 01, 0 \cdot 98] >, < x_8, [0 \cdot 03, 0 \cdot 00, 0 \cdot 97] > \end{array} \right\}$$

$$F_{T_7} = \left\{ \begin{array}{c} < x_1, [0 \cdot 18, 0 \cdot 00, 0 \cdot 82] >, < x_2, [0 \cdot 00, 0 \cdot 01, 0 \cdot 99] >, < x_3, [0 \cdot 04, 0 \cdot 00, 0 \cdot 96] >, \\ < x_4, [0 \cdot 00, 0 \cdot 02, 0 \cdot 98] >, < x_5, [0 \cdot 05, 0 \cdot 01, 0 \cdot 94] >, < x_6, [0 \cdot 04, 0 \cdot 01, 0 \cdot 95] >, \\ < x_7, [0 \cdot 44, 0 \cdot 10, 0 \cdot 46] >, < x_8, [0 \cdot 17, 0 \cdot 03, 0 \cdot 80] > \end{array} \right\}$$

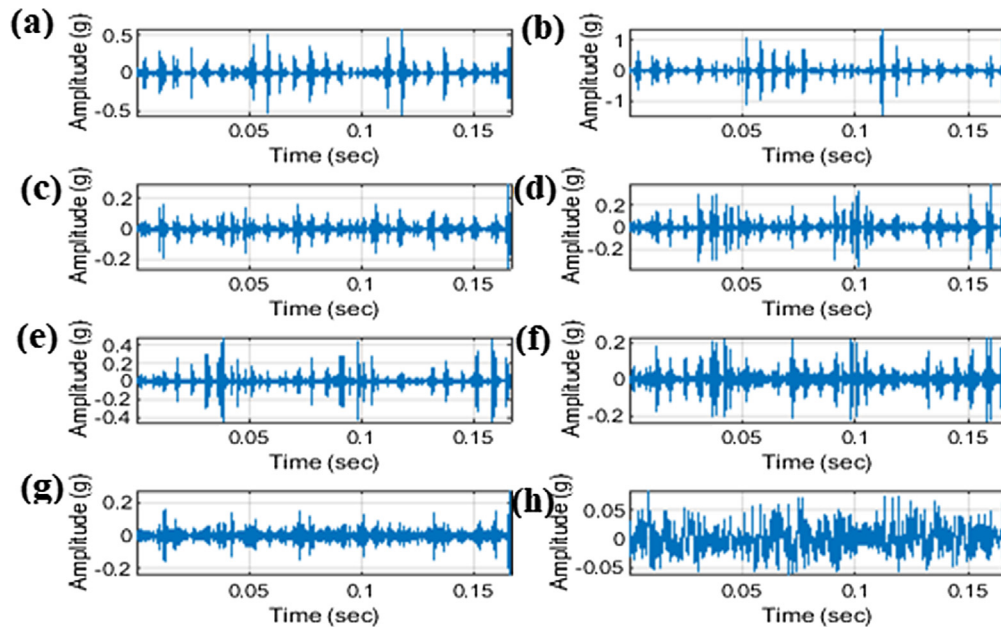**Fig. 16.** Sub-frequency bands under inner race defect condition: $(a) y_{3,7} (b) y_{3,6} (c) y_{3,5} (d) y_{3,4} (e) y_{3,3} (f) y_{3,2} (g) y_{3,1} (h) y_{3,0}$.

In short, the defined values of real testing samples can be finally represented into the form of SVNSs as $F_{T_j}(j = 4, 5, 6, 7) = \left\{ < x_i, \left[\tilde{\mu}_{F_{T_j}}(x_i), \tilde{i}_{F_{T_j}}(x_i), \tilde{f}_{F_{T_j}}(x_i) \right] > \right\}; (i = 1, 2, 3, .., 8).$

The SVNCE values $_{\text{SVNCE}}K\left(A_K, F_{T_j}\right)\left(A_K, F_{T_j}\right)$ between real testing samples $F_{T_j}(j = 4, 5, 6, 7)$ and various fault types $A_K(K = 4, 5, 6, 7)$ can be calculated using Eq. (10). Using minimum/maximum argument Principle, the fault diagnosis order, fault condition identified and actual fault condition of various knowledge of fault types obtained by the proposed SVNCE measure as well as by the existing method [21] are represented below (Table 12).

5.2. Diagnosis results and comparative analysis

The diagnosis can be carried out by computing minimum SVNCE values between the real testing samples $F_{T_j}(j = 4, 5, 6, 7)$ and various knowledge of fault types $A_K(K = 4, 5, 6, 7)$ as shown in Table 12, the results of which provide us the information that the proposed SVNCE measure $_{\text{SVNS}}K\left(A_K, F_{T_j}\right)(j = 4, 5, 6, 7)$ returns accurate fault diagnosis order.

Diagnosis results 1. For the real testing sample F_{T_4}, the minimum value of $_{\text{SVNS}}K\left(A_K, F_{T_4}\right)$ is 0.3900 which, according to minimum argument principle, corresponds to the normal condition A_7. Also, during inspection of bearing, it was found that bearing was healthy. Also, the existing method [21] based on SNSs gives similar results in this case.

Diagnosis result 2. For the real testing sample F_{T_4}, the minimum value of $_{\text{SVNS}}K\left(A_K, F_{T_5}\right)$ is 0.4262 which, according to minimum argument principle, corresponds to the fault type A_5 which indicates defect on the roller of the bearing. Thus, correctly identifies the defect.

On another hand, the maximum value $M_{\text{SNS}}\left(A_K, F_{T_5}\right)$ is 0.7118 which, according to maximum argument principle, corresponds to the fault type A_7 which indicates inner race defect in the bearing. Thus existing method [21] based on SNSs mistakenly identifies roller defect as inner race defect.

Diagnosis result 3. The minimum SVNCE value between the real testing sample F_{T_6} and $A_K(K = 4, 5, 6, 7)$ is 0.0368, which, according to minimum argument principle, corresponds to the condition type A_6 which indicates outer race defect in the bearing. Furthermore, during checking of bearing, we discover that the
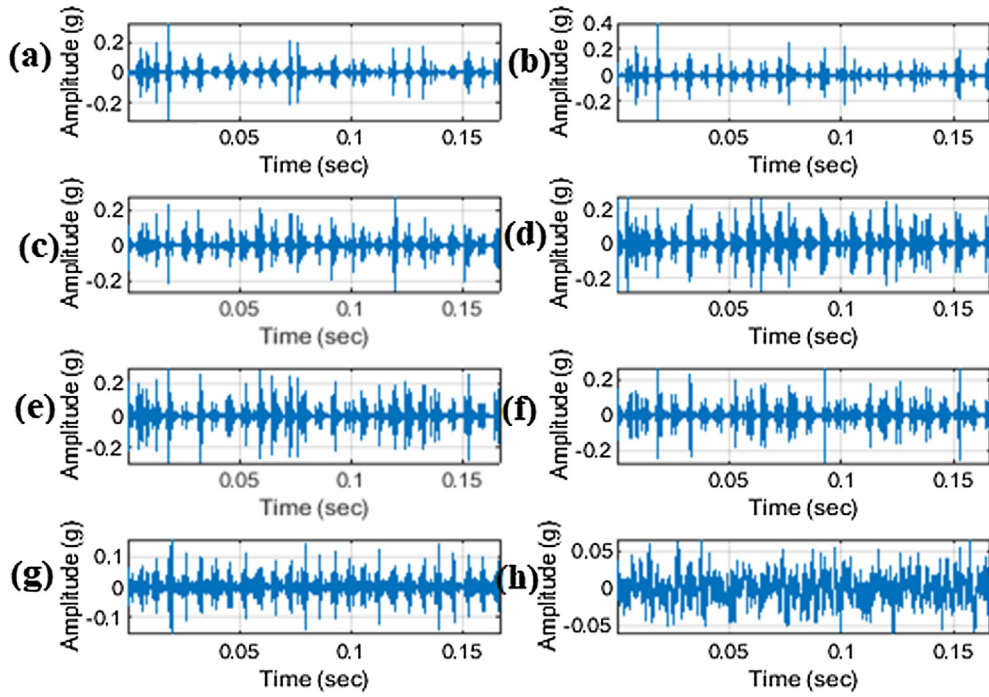
Fig. 17. Sub-frequency bands under an outer race defect condition: $(a)\,y_{3,7}\,(b)\,y_{3,6}\,(c)\,y_{3,5}\,(d)\,y_{3,4}\,(e)\,y_{3,3}\,(f)\,y_{3,2}\,(g)\,y_{3,1}\,(h)\,y_{3,0}$.
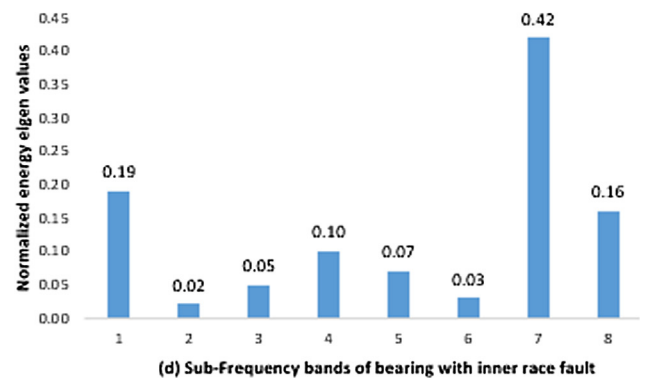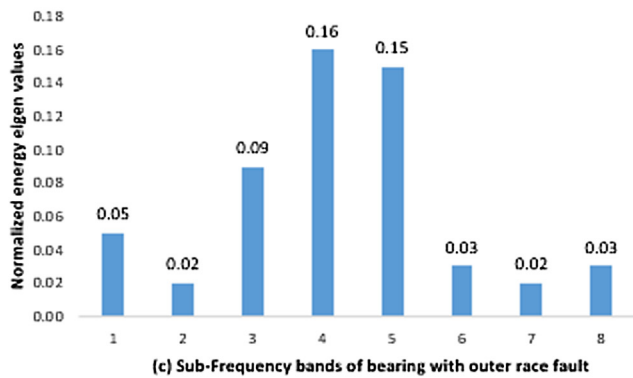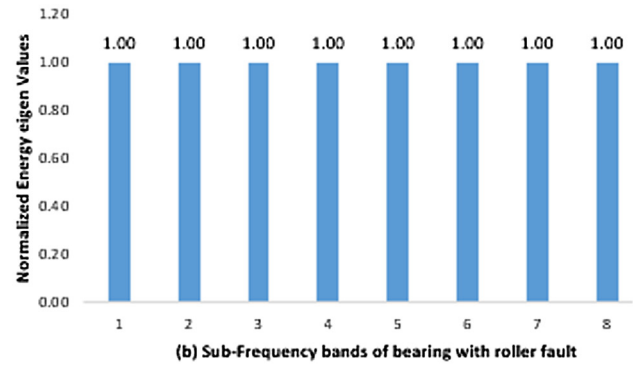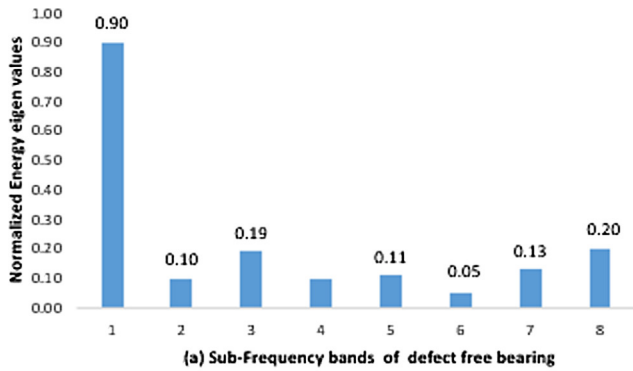

Fig. 18. Energy Histograms of (a) defect free bearing (b) bearing with faults on its roller (c) bearing with faults on its outer race and (d) bearing with faults on its inner race.

bearing was damaged and it was having defect on its outer race. The existing method [21] based on SNSs also identifies this fault as outer race fault.

Diagnosis results 4. For the real testing sample F_{T_6}, the minimum value of $_{SVNS}K(A_K, F_{T_7})$ is 0.0658 which, according to minimum argument principle, corresponds to the fault type A_7 which

Table 10
Energy interval ranges of eight sub-frequency bands.

Fault Types	Energy in each sub-frequency band							
	P_3^{*0}	P_3^{*1}	P_3^{*2}	P_3^{*3}	P_3^{*4}	P_3^{*5}	P_3^{*6}	P_3^{*7}
A_4: Defect Free	[0.74 0.90]	[0.08 0.10]	[0.11 0.19]	[0.05 0.10]	[0.05 0.11]	[0.04 0.05]	[0.07 0.13]	[0.10 0.20]
A_5: Roller	[0.63 1.00]	[0.48 1.00]	[0.65 1.00]	[0.46 1.00]	[0.45 1.00]	[0.44 1.00]	[0.31 1.00]	[0.22 1.00]
A_6: Outer race	[0.00 0.05]	[0.01 0.02]	[0.05 0.09]	[0.05 0.16]	[0.05 0.15]	[0.02 0.03]	[0.00 0.02]	[0.00 0.03]
A_7: Inner race	[0.10 0.19]	[0.01 0.02]	[0.00 0.05]	[0.03 0.10]	[0.00 0.07]	[0.00 0.03]	[0.15 0.42]	[0.06 0.16]

Table 11
Energy interval ranges of typical fault types at eight sub-frequency band represented in the form of SVNSs.

	Energy in each frequency Band							
Fault Types	P_3^{*0}	P_3^{*1}	P_3^{*2}	P_3^{*3}	P_3^{*4}	P_3^{*5}	P_3^{*6}	P_3^{*7}
A_4	[0.74 0.16 0.10]	[0.08 0.02 0.90]	[0.11 0.08 0.81]	[0.05 0.05 0.90]	[0.05 0.06 0.89]	[0.04 0.01 0.95]	[0.07 0.06 0.13]	[0.10 0.10 0.80]
A_5	[0.63 0.37 0.00]	[0.48 0.52 0.00]	[0.65 0.35 0.00]	[0.46 0.54 0.00]	[0.45 0.55 0.00]	[0.44 0.56 0.00]	[0.31 0.69 0.00]	[0.22 078 0.00]
A_6	[0.00 0.05 0.95]	[0.01 0.01 0.98]	[0.05 0.04 0.91]	[0.05 0.11 0.84]	[0.05 0.10 0.85]	[0.02 0.01 0.97]	[0.00 0.02 0.98]	[0.00 0.03 0.97]
A_7	[0.10 0.09 0.81]	[0.01 0.01 0.98]	[0.00 0.05 0.95]	[0.03 0.04 0.90]	[0.00 0.07 0.93]	[0.00 0.03 0.97]	[0.15 0.27 0.58]	[0.06 0.10 0.84]

Table 12
Fault diagnosis order obtained by the proposed method based on SVNSs and the existing method based on SNSs [20].

Existing method based upon SNSs

Measure	Correlation coefficient Values				Fault diagnosis order	Fault condition identified	Actual fault condition
	A_1	A_2	A_3	A_4			
$M_{SNS}(A_K, F_{T_1})$	0.8999	0.4161	0.8463	0.8571	$A_4 \to A_7 \to A_6 \to A_5$	Defect Free	Defect Free
$M_{SNS}(A_K, F_{T_2})$	0.6755	0.6829	0.7118	0.3652	$A_6 \to A_5 \to A_4 \to A_7$	Outer race	Roller
$M_{SNS}(A_K, F_{T_3})$	0.7199	0.2813	0.9581	0.8871	$A_6 \to A_7 \to A_4 \to A_5$	Outer race	Outer race
$M_{SNS}(A_K, F_{T_4})$	0.7827	0.3561	0.8832	0.9180	$A_7 \to A_6 \to A_4 \to A_5$	Inner Race	Inner Race

Proposed method based upon SVNSs

Measure	SVNCE Values				Fault diagnosis order	Fault condition identified	Actual fault condition
	A_1	A_2	A_3	A_4			
$_{SVNS}K(A_K, F_{T_1})$	0.0691	1.4677	0.2656	0.1787	$A_4 \to A_7 \to A_6 \to A_5$	Defect Free	Defect Free
$_{SVNS}K(A_K, F_{T_2})$	0.8334	0.2683	0.4380	0.4262	$A_5 \to A_7 \to A_6 \to A_4$	Roller	Roller
$_{SVNS}K(A_K, F_{T_3})$	0.3994	2.1184	0.0368	0.1527	$A_6 \to A_7 \to A_4 \to A_5$	Outer race	Outer race
$_{SVNS}K(A_K, F_4)$	0.2009	1.8463	0.1913	0.0658	$A_7 \to A_6 \to A_4 \to A_5$	Inner Race	Inner Race

indicates inner race defect in the bearing. Also, during inspection of bearing, it was found that bearing was damaged, and it was having defect on its inner race. The existing method [21] based on SNSs also identifies this fault as inner race fault.

5.3. Fault identification accuracy

The fault identification accuracy of the proposed method, in this case, is 100% (Table 13) and is compared with the existing method based on SNS [21]. The comparison is presented in Table 13. The fault identification accuracy achieved using the existing method based on SNSs is **90%** which is less than **100%** as obtained by the proposed method based on SVNSs.

5.4. Validity test

For demonstrating the effectiveness and validity of the proposed SVNCE measure under testing criteria as suggested by [27], we have

inter-changed the degree of true and falsity membership of each non-optimal (A_4) and worse alternative (A_5) of the real testing sample F_{T_6}. The new SVNCE values of $_{SVNS}K(A_K, F_{T_5})$ and $M_{SNS}(A_K, F_{T_5})$ along with the fault diagnosis order, non-optimal and worse alternatives of all the four kinds of familiar faults types are again calculated using Eq. (10) and are provided in Table 14.

A comparative analysis of the results of Tables 12 and 14 reveals that for the real testing sample F_{T_5}, the fault diagnosis order returned by the proposed SVNCE measure is $A_5 \to A_7 \to A_6 \to A_4$ whereas the non-optimal and worse alternatives are A_6 and A_4 respectively. Under testing criterion [27], the proposed SVNCE measure holds the same optimal fault type selection. The non-optimal and worse alternatives, which are A_4 and A_6 now have been inter-changed. This indicates that the proposed SVNCE measure based on SVNSs is capable for holding the fault types selection. On another hand, the existing method [21] based on SNNs fails to hold the optimal fault type selection under testing criteria [27], which indicates that the existing method [21] hides some useful evalua-

Table 13
Fault identification accuracy of the proposed method and the existing Method based on **SNSs** [21].

Model	Accuracy %				Overall accuracy %
	Defect free	Fault on roller	Outer race fault	Inner race fault	
Existing method based on SNSs [15]	100	60	100	100	90
Proposed method based on SVNSs	100	100	100	100	100

Table 14
Fault diagnosis order obtained by the proposed method and the existing method based on SNSs [21] under testing criteria [21].

Existing method based upon SNSs

Measure	Correlation coefficient Values				Fault diagnosis order	Non-optimal, Worse Alternative
	A_1	A_2	A_3	A_4		
$M_{SNS}(A_K, F_{T_1})$	0.8999	0.5762	0.3154	0.8571	$A_4 \rightarrow A_7 \rightarrow A_5 \rightarrow A_5$	A_5, A_6
$M_{SNS}(A_K, F_{T_2})$	0.6751	0.6755	0.6829	0.7118	$A_7 \rightarrow A_6 \rightarrow A_5 \rightarrow A_4$	A_5, A_4
$M_{SNS}(A_K, F_{T_3})$	0.2646	0.5634	0.9581	0.8871	$A_6 \rightarrow A_7 \rightarrow A_5 \rightarrow A_4$	A_5, A_4
$M_{SNS}(A_K, F_{T_4})$	0.3030	0.6245	0.8458	0.8970	$A_7 \rightarrow A_6 \rightarrow A_5 \rightarrow A_4$	A_5, A_4

Proposed method based upon SVNSs

Measure	SVNCE Values				Fault diagnosis order	Non-optimal, Worse Alternative
	A_1	A_2	A_3	A_4		
$_{SVNS}K(A_K, F_{T_1})$	0.0691	0.07089	1.5832	0.1787	$A_4 \rightarrow A_7 \rightarrow A_5 \rightarrow A_6$	A_6, A_5
$_{SVNS}K(A_K, F_{T_2})$	0.6058	0.2683	1.0026	0.4262	$A_5 \rightarrow A_7 \rightarrow A_4 \rightarrow A_6$	A_4, A_6
$_{SVNS}K(A_K, F_{T_3})$	1.4137	0.8909	0.0368	0.1527	$A_6 \rightarrow A_7 \rightarrow A_5 \rightarrow A_4$	A_5, A_4
$_{SVNS}K(A_K, F_4)$	1.3899	0.7568	0.1913	0.0658	$A_7 \rightarrow A_6 \rightarrow A_5 \rightarrow A_4$	A_5, A_4

Table 15
Fault diagnosis order obtained by the proposed method and the existing method based on SNSs [21] under sensitive analysis.

Existing method based upon SNSs

Measure	Correlation coefficient Values				Fault diagnosis order	Non-optimal, Worse Alternative
	A_1	A_2	A_3	A_4		
$M_{SNS}(A_K, F_{T_1})$	0.8999	0.4174	0.8463	0.8583	$A_4 \rightarrow A_7 \rightarrow A_6 \rightarrow A_5$	A_6, A_5
$M_{SNS}(A_K, F_{T_2})$	0.7425	0.6254	0.7009	0.4371	$A_4 \rightarrow A_6 \rightarrow A_5 \rightarrow A_7$	A_5, A_7
$M_{SNS}(A_K, F_{T_3})$	0.7211	0.2646	0.9594	0.8883	$A_6 \rightarrow A_7 \rightarrow A_4 \rightarrow A_5$	A_4, A_5
$M_{SNS}(A_K, F_{T_4})$	0.7839	0.3534	0.8844	0.9193	$A_7 \rightarrow A_6 \rightarrow A_5 \rightarrow A_4$	A_5, A_4

Proposed method based upon SVNSs

Measure	SVNCE Values				Fault diagnosis order	Non-optimal, Worse Alternative
	A_1	A_2	A_3	A_4		
$_{SVNS}K(A_K, F_{T_1})$	0.0692	1.4677	0.2657	0.1782	$A_4 \rightarrow A_7 \rightarrow A_6 \rightarrow A_5$	A_6, A_5
$_{SVNS}K(A_K, F_{T_2})$	0.8312	0.2672	0.4391	0.4256	$A_5 \rightarrow A_7 \rightarrow A_6 \rightarrow A_4$	A_6, A_4
$_{SVNS}K(A_K, F_{T_3})$	0.3984	2.1027	0.0357	0.1502	$A_6 \rightarrow A_7 \rightarrow A_4 \rightarrow A_5$	A_4, A_5
$_{SVNS}K(A_K, F_4)$	0.2011	1.8403	0.1915	0.0653	$A_7 \rightarrow A_6 \rightarrow A_4 \rightarrow A_5$	A_4, A_5

tion information of fault types and thus affects the diagnosis analysis resulting in the distortion phenomenon. It is therefore concluded that the final ranking for the real testing sample F_{T_4} is $A_4 \rightarrow A_7 \rightarrow A_6 \rightarrow A_5$, for F_{T_5} is $A_5 \rightarrow A_7 \rightarrow A_6 \rightarrow A_4$, for F_{T_6} is $A_6 \rightarrow A_7 \rightarrow A_4 \rightarrow A_5$ and for F_{T_7} is $A_7 \rightarrow A_6 \rightarrow A_4 \rightarrow A_5$ respectively.

5.5. Sensitive Analysis.

For the sensitive analysis of the proposed SVNCE measure, we have slightly changed the values $< x_6, [0 \cdot 04, 0 \cdot 01, 0 \cdot 95] >$ of the real testing samples F_{T_4} to $< x_6, [0 \cdot 04, 0 \cdot 02, 0 \cdot 95] >$, $< x_8, [0 \cdot 02, 0 \cdot 16, 0 \cdot 82] >$ of the real testing samples F_{T_5} to $< x_8, [0 \cdot 03, 0 \cdot 16, 0 \cdot 82] >$, $< x_6, [0 \cdot 02, 0 \cdot 00, 0 \cdot 98] >$ of the real testing samples F_{T_6} to $< x_6, [0 \cdot 02, 0 \cdot 01, 0 \cdot 98] >$, and $< x_6, [0 \cdot 04, 0 \cdot 01, 0 \cdot 95] >$ of the real testing samples F_{T_7} to $< x_6, [0 \cdot 04, 0 \cdot 02, 0 \cdot 95] >$ respectively. Next, we have re-calculated SVNCE values $_{SVNS}K(A_K, F_{T_j})(j = 4, 5, 6, 7)$ by using equation (10) and the fault diagnosis order, non-optimal and worse alternatives of all four kind of familiar faults types are represented in Table 15. Comparing the results of Tables 11 and 15, we have seen that, under sensitive analysis, the fault diagnosis order, non-optimal and worse alternatives of various real testing samples returned by the proposed method based upon SVNSs do not change. We have also re-calculated the new values of $_{SNS}M(A_K, F_{T_j})(j = 4, 5, 6, 7)$ and the results are displayed in Table 15. It is therefore concluded that the proposed method based on SVNSs is not sensitive since it holds the same optimal, non-optimal and worse alternative selection under sensi-

tive analysis. But, on another hand, the existing method [21] based on SNSs gives fails to hold the optimal fault type selection under sensitive analysis (For the real testing samples F_{T_5}).

6. Conclusion

In this study, we have been able to develop a novel symmetric single valued neutrosophic cross entropy (SVNCE) measure based upon a newly developed symmetric measure of fuzzy cross entropy. The advantage of the symmetric nature of the proposed SVNCE measure is that it can be applied more suitably for further mathematical treatments in certain situations where membership functions of asymmetrical phenomenon may produce undefined or meaningless results. The developed method is applied to identify faults of (a) cylindrical roller bearing installed in the customized test rig and (b) bearing of axial pump. The concluded results reveal that the fault identification accuracy of the existing method based upon simplified neutrosophic sets (SNSs) is much less (**90%**). On another hand, the newly developed method can identify every fault with an accuracy of **100%**. Moreover, under sensitive analysis, the proposed SVNCE measure based upon single valued neutrosophic sets (SVNSs) is capable for holding the fault types selection. It is therefore concluded that, the proposed method based upon SVNSs offers consistent and remarkable diagnosis information for the main faults of the cylindrical rolling bearing as well as axial pump bearing under consideration. This method is suitable for working at constant speed. For effective working at varying speed, this method requires removal of effect of speed by applying suitable processing.

In future, we wish to extend our method for the identification and prognosis of defects in different components such as gear, engine and rotor.

Declaration of Competing Interest

The authors declare that they have no known competing financial interests or personal relationships that could have appeared to influence the work reported in this paper.

Acknowledgements

References

[1] Z. Duan, T. Wu, S. Guo, et al., Development and trend of condition monitoring and fault diagnosis of multi-sensors information fusion for rolling bearings: a review, Int. J. Adv. Manuf. Technol. (2018), https://doi.org/10.1007/s00170-017-1474-8.

[2] M.-K. Liu, P.-Y. Weng, Fault diagnosis of ball bearing elements: a generic procedure based on time-frequency analysis, Meas. Sci. Rev. (2019), https://doi.org/10.2478/msr-2019-0024.

[3] A. Głowacz, Z. Głowacz, Recognition of rotor damages in a DC motor using acoustic signals, Bull. Polish. Acad. Sci. Tech. Sci. (2017), https://doi.org/10.1515/bpasts-2017-0023.

[4] L.A. Zadeh, Fuzzy sets, Inf. Control. 8 (1965) 338–353.

[5] K.T. Atanassov, Intuitionistic fuzzy sets, Fuzzy Sets Syst. 20 (1) (1986) 87–96.

[6] L.L. Jiang, H.K. Yin, X.J. Li, S.W. Tang, Fault diagnosis of rotating machinery based on multisensor information fusion using SVM and time-domain features, Shock Vib. 8 (2014), Article ID 418178,8 pages.

[7] A. Kumar, R. Kumar, Time-frequency analysis and support vector machine in automatic detection of defect from vibration signal of centrifugal pump, Measurement 108 (2017) 119–133.

[8] A. Kumar, R. Kumar, Adaptive artificial intelligence for automatic identification of defect in the angular contact bearing, Neural Comput. Appl. 29 (2018) 277–287.

[9] D. Wang, Y. Zhao, C. Yi, K.-L. Tsui, J. Lin, Sparsity guided empirical wavelet transform for fault diagnosis of rolling bearings, Mech. Syst. Sig. Process. 101 (2018) 292–308.

[10] Mohamed Zair, Chemseddine Rahmoune and Djamel Benazzouz (2018), "Multi-Fault Diagnosis of Rolling Bearing Using Fuzzy Entropy of Empirical Mode Decomposition, Principal Component Analysis, and SOM Neural Network", Journal of Mechanical Engineering Science, pp.1-12..

[11] Fu. Ling, Zhengyon He, Ruikum Mai, Zhiqian Bo, Approximate entropy and its application to fault detection and identification in power swing, IEEE Trans. (2009) 1–8.

[12] Yu. Bing, Dongdong Liu, Tianhong Zhang, Fault diagnosis for micro-gas turbine engine sensors via wavelet entropy, Sensors 11 (2011) 9928–9941.

[13] A. Stief, J.R. Ottewill, J. Baranowski, M. Orkisz, A PCA and two-stage bayesian sensor fusion approach for diagnosing electrical and mechanical faults in induction motors, IEEE Trans. Ind. Electron. (2019), https://doi.org/10.1109/tie.2019.2891453.

[14] A. Glowacz, W. Glowacz. Vibration-Based Fault Diagnosis of Commutator Motor SHOCK AND VIBRATION. 2018, Article ID 7460419. https://doi.org/10.1155/2018/7460419..

[15] C. Bandit, B. Pompe, Permutation entropy: a natural complexity measure for time series, Phys. Rev. Lett. 88 (2002) 174102.

[16] Ye Tian, Zili Wang, Lu. Chen, Self-adaptive bearing fault diagnosis based on permutation entropy and manifold-based dynamic time warping, Mech. Syst. Signal Process. (2016) 1–16.

[17] L.Y. Zhao, L. Wang, R.Q. Yan, Rolling bearing fault diagnosis based on wavelet packet decomposition and multiscale permutation entropy, Entropy 17 (9) (2015) 6447–6461.

[18] B.C. Cuong, Picture fuzzy sets -first result, part 1, in seminar "neuro-fuzzy systems with applications". Tech. rep, Institute of Mathematics, Hanoi, 2013.

[19] F. Smarandache, Neutrosophy: neutrosophic probability, set and logic, American Research Press Rehoboth, DE, USA, 1998.

[20] Jiang Weng, Yehang Shou, A novel single valued neutrosophic set, similarity measure and its applications to multicriteria decision making methods, Symmetry 9 (127) (2017) 1–14.

[21] L.L. Shi, Correlation coefficient of simplified neutrosophic sets for bearing fault diagnosis, Shock Vib. 20 (2) (2016) 1–11.

[22] Y. Zhang, Y. Zhao, S. Gao, (2019). A Novel Hybrid Model for Wind Speed Prediction Based on VMD and Neural Network Considering Atmospheric Uncertainties. 10.1109/ACCESS.2019.2915582..

[23] Y. Zhang, B. Chen, G. Pan, Y. Zhao, A novel hybrid model based on VMD-WT and PCA-BP-RBF neural network for short-term wind speed forecasting, Energy Convers Manag. (2019), https://doi.org/10.1016/j.enconman.2019.05.005.

[24] D. Bhandari, N.R. Pal, Some new information measures for fuzzy sets, Inf. Sci. 67 (1993) 209–226.

[25] X.G. Shang, W.S. Jiang, A note on fuzzy information measures, Pattern Recogn. Lett. 18 (1997) 425–432.

[26] L.L. Shi, J. Ye, Study on fault diagnosis of turbine using an improved cosine similarity measure of vague sets, J. Appl. Sci. 13 (10) (2013) 1781–1786.

[27] X. Wang, E. Triantaphyllou, Ranking irregularities when evaluating alternatives by using some ELECTRE methods" Omega International Journal of management, Science 36 (2008) 4563.